

## Quantum fluctuations and CMB anisotropies in one-bubble open inflation models

Kazuhiro Yamamoto<sup>1</sup>, Misao Sasaki<sup>2</sup> and Takahiro Tanaka<sup>2</sup>

<sup>1</sup> *Department of Physics, Hiroshima University  
Higashi-Hiroshima 739, Japan*

<sup>2</sup> *Department of Earth and Space Science,  
Osaka University, Toyonaka 560, Japan*

We first develop a method to calculate a complete set of mode functions which describe the quantum fluctuations generated in one-bubble open inflation models. We consider two classes of models. One is a single scalar field model proposed by Bucher, Goldhaber and Turok and by us as an example of the open inflation scenario, and the other is a two-field model such as the “supernatural” inflation proposed by Linde and Mezhlumian. In both cases we assume the difference in the vacuum energy density between inside and outside the bubble is negligible. There are two kinds of mode functions. One kind has usual continuous spectrum and the other has discrete spectrum with characteristic wavelengths exceeding the spatial curvature scale. The latter can be further divided into two classes in terms of its origin. One is called the de Sitter super-curvature mode, which arises due to the global spacetime structure of de Sitter space, and the other is due to fluctuations of the bubble wall. We calculate the spectrum of quantum fluctuations in these models and evaluate the resulting large angular scale CMB anisotropies. We find there are ranges of model parameters that are consistent with observed CMB anisotropies.

### I. INTRODUCTION

Motivated by observations that we may live in a low density universe [1–3], several authors have considered a possible scenario which realizes an open universe ( $\Omega_0 < 1$ ) in the context of inflationary cosmology [4–7]. In contrast to the standard inflation models which predict a spatially flat universe ( $\Omega_0 = 1$ ), this scenario predicts an universe with spatially negative curvature. In this scenario, the nucleation of a vacuum bubble plays an essential role. In general, the bubble nucleation process is described by the bounce solution with  $O(4)$ -symmetry, which is a non-trivial classical solution of the field equation in Euclidean spacetime [8,9]. Then the expanding bubble after nucleation is described by the classical solution obtained by analytic continuation of the bounce solution to Lorentzian spacetime. Owing to the  $O(4)$ -symmetry of the bounce solution, the expanding bubble has the  $O(3,1)$ -symmetry. This implies that the system is homogeneous and isotropic on the hyperbolic time slicing inside the bubble and that the creation of one bubble can be regarded as the creation of an open universe.

To obtain a realistic model of an open universe, the flatness  $\Omega_0 \sim 1$  and the homogeneity and isotropy of the universe should be realized inside the bubble. This requirement can be satisfied by assuming, for example, a scalar field with a potential such as in the new inflation scenario but with a high potential barrier before the slow rolling inflationary phase [4,5]. In addition, the high potential barrier keeps the bubble collision rate small, hence the homogeneity and isotropy of the one-bubble universe is not disturbed by the other nucleated bubbles. Then the second inflation inside the bubble inflates the universe and explains the flatness  $\Omega_0 \sim 1$ . Linde and Mezhlumian has proposed another (perhaps more natural) model of open inflation by introducing two scalar fields [6,7], but the essential feature of scenario is the same as the former.

The interesting problem is the origin of fluctuations in this open inflationary scenario. Following the usual picture that quantum fluctuations of the scalar field generate the initial density perturbations, we need to investigate the

quantum state of the scalar field after bubble nucleation. According to previous investigations, the open inflation scenario shows interesting varieties of the fluctuations. The bubble nucleation process can excite fluctuations of the scalar field and may increase the power of density fluctuations on scale of spatial curvature [10,11]. Also it has been shown that peculiar discrete modes of fluctuations on super-curvature scale may exist [12] and contribute to cosmic microwave background (CMB) anisotropies in an open universe [5,13]. Very recently, generation of another type of super-curvature perturbations which originate from the bubble wall perturbations has been discussed [11,14,15].

In this paper, we develop a method to calculate these varieties of fluctuations in the open inflationary universe and evaluate the power spectrum of the resulting CMB anisotropies. In order to perform a detailed analysis of the power spectrum, it is necessary to specify the model to some extent. Here we consider two classes of models. One is a single scalar field model (Model A) proposed by Bucher, Goldhaber and Turok [4] and by ourselves [5]. The other is a two-field model (Model B) in which the false vacuum decay and inflation inside the bubble are governed by two different scalar fields, such as the supernatural inflation proposed by Linde and Mezhlumian [7]. For simplicity, we assume the difference in the vacuum energy density between inside and outside the bubble is negligible in both models. Our method is based on the formalism we developed previously for computing the mode functions during and after bubble nucleation [16,17,12].

This paper is organized as follows. In section 2 we describe our method to calculate quantum fluctuations of the inflaton field. We assume that the reaction to the geometry can be neglected, i.e., the nucleation occurs in the de Sitter spacetime background. Then, in section 3, we investigate the evolution of fluctuations inside the bubble in an open inflationary stage and derive the formulas to calculate the initial perturbation spectrum of the open universe and the resulting CMB anisotropies. In section 4 we evaluate the CMB anisotropies in two simple models and examine their viability. Section 5 is devoted to conclusion. We adopt the units  $c = \hbar = 1$ , and the bar denotes the complex conjugate.

## II. FORMALISM

In this section, we describe our formalism to investigate quantum field fluctuations inside a bubble. Pioneering work on the quantum state of a nucleating bubble was done by Rubakov [18], Kandrup [19], Vachaspati and Vilenkin [20]. Recently, we have developed a formalism to investigate the quantum state of a scalar field after false vacuum decay based on the WKB wave function of a multi-dimensional tunneling system [16,21]. The formalism has been applied to the bubble nucleation which occurs on the Minkowski background, and the spectrum of field fluctuations after the decay has been studied [10,11]. The basic formalism has been extended to the case in which the bubble nucleation occurs on the de Sitter spacetime [17]. There the effect of the non-trivial geometry of the instanton with gravity, i.e., the Coleman-De Luccia instanton [9] was taken into account. At that time, however, the appropriate set of the mode functions to describe the initial vacuum state, which is expected to be the Bunch-Davies vacuum due to the sufficient inflation before the tunneling, had not been known. Thus there was a technical difficulty in applying our formalism. Recently, we have succeeded in describing the Bunch-Davies vacuum state in the spatially open chart [12]. Thus this problem has been overcome. Combining the results in these two papers [17,12], we now have a tool to handle the quantum fluctuations after tunneling which includes the effect of the geometry of the Coleman-De Luccia instanton similar to the case in the Minkowski background [10].

In the present paper, we consider simple open inflation models in which the geometry of the Coleman-De Luccia instanton can be approximated by the pure de Sitter spacetime. That is we consider the case in which the potential energy difference between the two vacua of the tunneling field is small. We consider the action

$$S = \int \left( -\frac{1}{2} g^{\mu\nu} \partial_\mu \sigma \partial_\nu \sigma - V(\sigma) \right) \sqrt{-g} d^4x + \int \left( -\frac{1}{2} g^{\mu\nu} \partial_\mu \phi \partial_\nu \phi - U(\sigma, \phi) \right) \sqrt{-g} d^4x, \quad (2.1)$$

where the potential  $V(\sigma)$  is assumed to have the form as shown in Figs. 1(a), (b) to realize the false vacuum decay. As we mentioned above, we take account of the effect of gravity only as a curved background which is assumed to be de Sitter space. We denote the value of  $\sigma$  at the false vacuum by  $\sigma_F$ . The field  $\phi$  is the inflaton in the nucleated bubble. We divide them into two parts as  $\phi = \phi_B + \varphi$ .  $\phi_B$  is the semi-classical, spatially homogeneous part of the field and  $\varphi$  represents the quantum fluctuations around this background. We neglect the quantum fluctuations of  $\sigma$  and denote its  $O(4)$ -symmetric background by  $\sigma_B$ . Due to the  $O(4)$ -symmetry of the instanton,  $\sigma_B$  is a function of only one coordinate, say  $\tau$ . In addition, we assume  $\phi_B$  also respects the  $O(4)$ -symmetry. Thus a model we have in mind is a two-field one, with  $\phi_B$  being constant at  $\sigma_B = \sigma_F$ . Note that we can consider a single field model by identifying  $\varphi$  with the quantum fluctuations of  $\sigma$  and letting  $U(\sigma, \phi) = V''(\sigma)\phi^2/2$ .

With these assumptions, the action for  $\varphi$  reduces to

$$S_\varphi = \int \left( -\frac{1}{2} g^{\mu\nu} \partial_\mu \varphi \partial_\nu \varphi - \frac{1}{2} \mathcal{M}^2(\tau) \varphi^2 \right) \sqrt{-g} d^4x, \quad (2.2)$$

where

$$\mathcal{M}^2(\tau) = \frac{\partial^2 U}{\partial \phi^2}(\sigma_B(\tau), \phi_B(\tau)). \quad (2.3)$$

As noted above, in the case of a single field model,  $\phi_B$  and  $\mathcal{M}^2(\tau)$  in the following discussion should be replaced by  $\sigma_B$  and  $\frac{\partial^2 V}{\partial \sigma^2}(\sigma_B(\tau))$ , respectively.

Our formalism is summarized in the following. It is based on the WKB wave function which describes the tunneling decay in a multi-dimensional system [16,17]. The construction of the wave function was originally developed by Gervais and Sakita [22]. The wave functional is written in terms of the bounce solution  $\sigma_B$ , which gives the semi-classical picture of the nucleation and expanding bubble, and a set of mode functions which describe the quantum fluctuations  $\varphi$  on the bounce solution [16]. The boundary condition for these mode functions is determined from the fact that the wave function describes the false vacuum state at  $\sigma_B = \sigma_F$ . It then turned out that the procedure to obtain the appropriate set of mode functions is equivalent to finding out a complete set of them which are regular in one hemisphere of the Euclideanized de Sitter space [17,12]. That is, to find a complete set of mode functions  $v_{\mathbf{k}}$  which obey

$$\left[ \nabla^\mu \nabla_\mu - \mathcal{M}^2 \right] v_{\mathbf{k}}(t, \mathbf{x}) = 0, \quad (2.4)$$

in the Lorentzian region, and which are regular on the  $\text{Im } t < 0$  hemisphere. Here, it is important to note that ‘‘a complete set’’ means a set of all modes which are properly normalized by the Klein-Gordon norms on a Cauchy surface  $\Sigma$  of spacetime,

$$\begin{aligned} \langle v_{\mathbf{k}}, v_{\mathbf{k}'} \rangle &:= -i \int_{\Sigma} d\Sigma_\mu g^{\mu\nu} \{ v_{\mathbf{k}} \partial_\nu \bar{v}_{\mathbf{k}'} - (\partial_\nu v_{\mathbf{k}}) \bar{v}_{\mathbf{k}'} \} \\ &= \delta_{\mathbf{k}\mathbf{k}'}. \end{aligned} \quad (2.5)$$

Once they are obtained, the quantum fluctuations of the field are described by the ‘‘vacuum state’’,  $|\Psi\rangle$ , such that  $\hat{a}_{\mathbf{k}}|\Psi\rangle = 0$  for any  $\mathbf{k}$  where the fluctuating field is expressed as

$$\hat{\varphi}_H = \sum_{\mathbf{k}} (v_{\mathbf{k}} \hat{a}_{\mathbf{k}} + \bar{v}_{\mathbf{k}} \hat{a}_{\mathbf{k}}^\dagger), \quad (2.6)$$

in the Heisenberg representation, with  $\hat{a}_{\mathbf{k}}$  and  $\hat{a}_{\mathbf{k}}^\dagger$  being the annihilation and creation operators, respectively. Thus the mode functions  $v_{\mathbf{k}}$  play the role of the positive frequency functions.

To write down the equation for the mode functions, we introduce the coordinates in the de Sitter spacetime following Ref. [12]. The four-dimensional Euclidean de Sitter space is a four-sphere. The metric is represented as

$$ds_E^2 = H^{-2} d\tau^2 + a_E^2(\tau) (d\rho^2 + \sin^2 \rho d\Omega^2), \quad (2.7)$$

where  $-\pi/2 \leq \tau \leq \pi/2$ ,  $0 \leq \rho \leq \pi$  and  $a_E(\tau) = H^{-1} \cos \tau$ . The mode functions are required to be regular on the  $0 \leq \rho \leq \pi/2$  hemisphere.

The coordinate systems in the Lorentzian de Sitter space are obtained by analytic continuation as

$$\begin{aligned} t_R &= i(\tau - \pi/2) \quad (t_R \geq 0), \\ r_R &= i\rho \quad (r_R \geq 0), \\ t_C &= \tau \quad (\pi/2 \geq t_C \geq -\pi/2), \\ r_C &= i(\rho - \pi/2) \quad (\infty > r_C > -\infty), \\ t_L &= i(-\tau - \pi/2) \quad (t_L \geq 0), \\ r_L &= i\rho \quad (r_L \geq 0). \end{aligned} \quad (2.8)$$

we find that each set of these coordinates covers three distinct parts of the Lorentzian de Sitter spacetime, which we call the regions  $R$ ,  $C$ , and  $L$  (see Fig.2). The metrics in these three regions are given by

$$\begin{aligned} ds_R^2 &= -H^{-2} dt_R^2 + a^2(t_R) (dr_R^2 + \sinh^2 r_R d\Omega^2), \\ ds_C^2 &= H^{-2} dt_C^2 + a_E^2(t_C) (-dr_C^2 + \cosh^2 r_C d\Omega^2), \\ ds_L^2 &= -H^{-2} dt_L^2 + a^2(t_L) (dr_L^2 + \sinh^2 r_L d\Omega^2), \end{aligned} \quad (2.9)$$

respectively, where  $a(t) = H^{-1} \sinh t$ . We assign the region L to be in the false vacuum sea and the region R to describe the open universe inside the bubble.

The equation for the bounce in the Euclidean region is given by

$$\frac{H^2}{a_E^3} \frac{d}{d\tau} \left( a_E^3 \frac{d\sigma_B}{d\tau} \right) - V'(\sigma_B) = 0. \quad (2.10)$$

The equation in the Lorentzian region is given by the analytic continuation of the coordinates as specified in Eqs. (2.8). The fluctuation field  $\varphi$  obeys, in the Euclidean region,

$$\left[ \frac{1}{a_E^3} \frac{\partial}{\partial(H^{-1}\tau)} a_E^3 \frac{\partial}{\partial(H^{-1}\tau)} - \frac{1}{a_E^2} \mathbf{L}^2 - \mathcal{M}^2(\tau) \right] \varphi = 0, \quad (2.11)$$

where

$$\mathbf{L}^2 = -\frac{1}{\sin^2 \rho} \frac{\partial}{\partial \rho} \left( \sin^2 \rho \frac{\partial}{\partial \rho} \right) - \frac{\mathbf{L}_\Omega^2}{\sin^2 \rho}, \quad (2.12)$$

and  $\mathbf{L}_\Omega^2$  is the Laplacian on a unit two sphere.

Setting  $\varphi = a_E(\tau)^{-1} \chi_p(\tau) f_{pl}(\rho) Y_{lm}(\Omega)$ , the equations for  $\chi_p$  and  $f_{pl}$  become, respectively,

$$\left[ (1-x^2) \frac{d^2}{dx^2} - 2x \frac{d}{dx} + \frac{p^2}{1-x^2} + 2 - \frac{\mathcal{M}^2}{H^2} \right] \chi_p = 0, \quad (2.13)$$

where  $x = \sin \tau$ , and

$$\left[ -\frac{1}{\sin^2 \rho} \frac{\partial}{\partial \rho} \left( \sin^2 \rho \frac{\partial}{\partial \rho} \right) + \frac{l(l+1)}{\sin^2 \rho} + (p^2 + 1) \right] f_{pl} = 0. \quad (2.14)$$

The requirement that the mode functions be regular at  $\rho = r_L = r_R = 0$  fixes the form of  $f_{pl}$  to be [12]

$$\begin{aligned} f_{pl}(r) &= \frac{\Gamma(ip+l+1)}{\Gamma(ip+1)} \frac{p}{\sqrt{\sinh r}} P_{ip-1/2}^{-l-1/2}(\cosh r) \\ &= (-1)^l \sqrt{\frac{2}{\pi}} \frac{\Gamma(-ip+1)}{\Gamma(-ip+l+1)} \sinh^l r \frac{d^l}{d(\cosh r)^l} \left( \frac{\sin pr}{\sinh r} \right), \end{aligned} \quad (2.15)$$

where  $r = ip$  in the Euclidean region. The gamma function factor in front is attached so that the functions  $Y_{plm}(r, \Omega) := f_{pl}(r) Y_{lm}(\Omega)$  become properly normalized harmonics on the hyperbolic slices in the region R or L:

$$\int_0^\infty dr \sinh^2 r \int d\Omega Y_{plm}(r, \Omega) \overline{Y_{p'l'm'}(r, \Omega)} = \delta(p-p') \delta_{ll'} \delta_{mm'}. \quad (2.16)$$

As we have noted before, a complete set of mode functions should be properly normalized on a Cauchy surface. Therefore we consider the mode functions in the region C, since it is the region in which complete Cauchy surfaces exist. It should be noted that  $f_{pl}$  play the role of the positive frequency functions there. Then the remaining tasks are (1) to find the possible spectrum of  $p$  that may give finite Klein-Gordon norms and (2) to properly normalize the mode functions if they are normalizable.

To accomplish the first task, we now consider the equation for  $\chi_p$ , (2.13). In the region C, the equation for  $\chi_p$  remains the same because  $t_C = \tau$ . Introducing the conformal coordinate  $\xi$  by the relation  $x = \sin \tau = \tanh \xi$ , the metric in the region C becomes

$$ds^2 = a_E^2(\xi) (-dr_C^2 + d\xi^2 + \cosh^2 r_C d\Omega^2), \quad (2.17)$$

where  $a_E = (H \cosh \xi)^{-1}$  and Eq. (2.13) is rewritten as

$$\left[ -\frac{d^2}{d\xi^2} + U(\xi) \right] \chi_p = p^2 \chi_p, \quad (2.18)$$

where

$$U(\xi) = \frac{\mathcal{M}^2/H^2 - 2}{\cosh^2 \xi}. \quad (2.19)$$

This resembles the Schrödinger equation with the potential  $U(\xi)$  and the energy  $E = p^2$ . Thus finding possible values of  $p$  is equivalent to solving the eigenvalue problem of the above equation. Since  $U(\xi) \rightarrow 0$  at  $\xi \rightarrow \pm\infty$ , the spectrum of modes is continuous for  $p^2 \geq 0$ . On the other hand, if  $\mathcal{M}^2 < 2H^2$  for some interval of  $\xi$ , the potential has a valley and some discrete modes which correspond to bound states may appear for  $p^2 = -\Lambda^2 < 0$ . In fact, it has been shown that there exists a discrete eigenvalue of  $\Lambda^2$  in two different simple cases. One is a mode which appears when we consider a scalar field with a constant small mass ( $< \sqrt{2H^2}$ ) on the de Sitter spacetime [12]. Its origin is intrinsic to the spacetime structure of the de Sitter universe. As long as the volume with  $\mathcal{M}^2 < 2H^2$  is large enough, an analogous mode is expected to exist in general. Let us call it the de Sitter super-curvature mode.\* The other is the mode that appears when we consider the fluctuations of the tunneling field itself [11]. It describes the fluctuation of the wall. Since it turns out that the analysis of the wall fluctuation mode can be simplified compared with the other discrete modes, below we consider the continuous modes, the de Sitter super-curvature mode, and the wall fluctuation mode separately in sequence. For simplicity, we assume that  $\mathcal{M}$  is constant in the regions R and L and set

$$\mathcal{M}^2 = \begin{cases} m^2 & \text{in R,} \\ M^2 & \text{in L,} \end{cases} \quad (2.20)$$

in the following discussion.

### A. Continuous modes

We first consider the continuous spectrum mode functions of  $p^2 > 0$ . For these modes, it has been shown that the Klein-Gordon norms can be evaluated by the sum of those on the hyperbolic slices on the regions R and L [12]. Since in the regions R and L,  $\mathcal{M}^2$  is supposed to be constant,  $\chi_p$  is given by an associated Legendre function  $P_{\nu-1/2}^{ip}(z)$  or  $P_{\nu-1/2}^{-ip}(z)$  with  $\nu = \sqrt{9/4 - \mathcal{M}^2/H^2}$ . To construct the normalized mode functions, we begin with the following mode functions in the regions R and L:

$$\begin{aligned} u_{plm}^{(R)} &= \frac{1}{a(t_R)} \chi_p^{(R)}(t_R) Y_{plm}(r_R, \Omega), \\ u_{plm}^{(L)} &= \frac{1}{a(t_L)} \chi_p^{(L)}(t_L) Y_{plm}(r_L, \Omega), \end{aligned} \quad (2.21)$$

where

$$\begin{aligned} \chi_p^{(R)}(t_R) &= P_{\nu'}^{ip}(z_R); & z_R &= \cosh t_R, \\ \chi_p^{(L)}(t_L) &= P_{\mu'}^{ip}(z_L); & z_L &= \cosh t_L, \end{aligned} \quad (2.22)$$

with  $\nu' = \sqrt{9/4 - m^2/H^2} - 1/2$  and  $\mu' = \sqrt{9/4 - M^2/H^2} - 1/2$ . The norms of these functions are given by

$$\begin{aligned} [(\chi_p^{(R)}, \chi_p^{(R)})]^{(R)} &:= i(z_R^2 - 1) \left\{ \frac{d\chi_p^{(R)}}{dz_R} \bar{\chi}_p^{(R)} - \chi_p^{(R)} \frac{d\bar{\chi}_p^{(R)}}{dz_R} \right\} = \frac{2}{\pi} \sinh \pi p, \\ [(\chi_p^{(L)}, \chi_p^{(L)})]^{(L)} &:= i(z_L^2 - 1) \left\{ \frac{d\chi_p^{(L)}}{dz_L} \bar{\chi}_p^{(L)} - \chi_p^{(L)} \frac{d\bar{\chi}_p^{(L)}}{dz_L} \right\} = \frac{2}{\pi} \sinh \pi p. \end{aligned} \quad (2.23)$$

If we analytically continue  $\chi_p^{(R)}$  to the region L by solving Eq. (2.18) in the region C,  $\chi_p^{(R)}$  will be expressed in terms of a linear combination of  $\chi_p^{(L)}$  and  $\chi_{-p}^{(L)}$ . Hence we consider the mode function,

$$\chi_p = \chi_p^{(R)} = \alpha_p \chi_{-p}^{(L)} + \beta_p \chi_p^{(L)}. \quad (2.24)$$

From the property of the analytic continuation [12] and the reality of the Eq. (2.18), there exists a symmetry,

---

\*The spatial harmonics behave as  $Y_{plm}(r) \propto e^{-r}$  for  $p^2 > 0$ . As  $r = 1$  corresponds to the scale of spatial curvature, fluctuations described by the harmonics with  $p^2 > 0$  represents those which decay exponentially on scales larger than the curvature scale. In contrast, harmonics with  $p^2 = -\Lambda^2 < 0$  behave as  $Y_{\Lambda lm} \propto e^{(\Lambda-1)r}$ , hence describe fluctuations over scales larger than the curvature scale [23,24]. The name ‘‘super-curvature’’ originates from this fact.

$$\begin{aligned}\bar{\chi}_p^{(R)} &= e^{-\pi p} \chi_{-p}^{(R)}, \\ \bar{\chi}_p^{(L)} &= e^{-\pi p} \chi_{-p}^{(L)},\end{aligned}\tag{2.25}$$

in the region C. Then we obtain

$$\bar{\alpha}_p = e^{-2\pi p} \alpha_{-p}, \quad \bar{\beta}_p = \beta_{-p}.\tag{2.26}$$

Further, defining the Wronskian by

$$((u, v)) := u \frac{dv}{d\xi} - \frac{du}{d\xi} v,\tag{2.27}$$

$\alpha_p$  and  $\beta_p$  are expressed as

$$\alpha_p = \frac{((\chi_p^{(L)}, \chi_p^{(R)}))}{((\chi_p^{(L)}, \chi_{-p}^{(L)}))}, \quad \beta_p = \frac{((\chi_p^{(R)}, \chi_{-p}^{(L)}))}{((\chi_p^{(L)}, \chi_{-p}^{(L)}))},\tag{2.28}$$

and we have

$$((\chi_p, \bar{\chi}_p)) = ((\chi_p^{(R)}, \bar{\chi}_p^{(R)})) = (e^{2\pi p} |\alpha_p|^2 - |\beta_p|^2) ((\bar{\chi}_p^{(L)}, \chi_p^{(L)})).\tag{2.29}$$

Also from the analytic continuation of the Eq. (2.23) we obtain

$$((\chi_p^{(R)}, \bar{\chi}_p^{(R)})) = ((\bar{\chi}_p^{(L)}, \chi_p^{(L)})).\tag{2.30}$$

Thus we find

$$X := |\beta_p|^2 = e^{2\pi p} |\alpha_p|^2 - 1.\tag{2.31}$$

Now define

$$[(\chi_1, \chi_2)] := [(\chi_1, \chi_2)]^{(R)} + [(\chi_1, \chi_2)]^{(L)},\tag{2.32}$$

which gives the contribution of the function  $\chi_p$  to the total Klein-Gordon norm. Then we have

$$\begin{aligned}K_{++} &:= [(\chi_p, \chi_p)] = \frac{4}{\pi} e^{-\pi p} \sinh^2 \pi p (1 + X), \\ K_{+-} &:= [(\chi_p, \chi_{-p})] = \frac{4}{\pi} e^{\pi p} \sinh^2 \pi p \alpha_p \beta_p, \\ K_{-+} &:= [(\chi_{-p}, \chi_p)] = \frac{4}{\pi} e^{\pi p} \sinh^2 \pi p \bar{\alpha}_p \bar{\beta}_p, \\ K_{--} &:= [(\chi_{-p}, \chi_{-p})] = \frac{4}{\pi} e^{\pi p} \sinh^2 \pi p (1 + X),\end{aligned}\tag{2.33}$$

and

$$|K_{+-}|^2 = \left( \frac{4}{\pi} \sinh^2 \pi p \right)^2 X(1 + X).\tag{2.34}$$

To find the orthonormalized mode functions, we must find a matrix  $M_{\sigma\sigma'}$  which diagonalizes the matrix  $K_{\sigma\sigma'}$  ( $\sigma, \sigma' = +, -$ ).<sup>†</sup> It can be chosen as

$$M_{\sigma\sigma'} = \begin{pmatrix} \frac{-K_{-+}}{\sqrt{|K_{+-}|^2 + (K_{++} - \lambda_+)^2}} & \frac{K_{++} - \lambda_+}{\sqrt{|K_{+-}|^2 + (K_{++} - \lambda_+)^2}} \\ \frac{-K_{-+}}{\sqrt{|K_{+-}|^2 + (K_{++} - \lambda_-)^2}} & \frac{K_{++} - \lambda_-}{\sqrt{|K_{+-}|^2 + (K_{++} - \lambda_-)^2}} \end{pmatrix},\tag{2.35}$$

---

<sup>†</sup>Instead of allowing  $p$  to have the range  $-\infty < p < \infty$ , we restrict it in the range  $0 < p < \infty$  but doubling the degrees of freedom with  $\sigma = \pm 1$ .

where  $\lambda_{\pm}$  are the eigenvalues of  $K_{\sigma\sigma'}$ ,

$$\lambda_{\pm} = \frac{1}{2} \left( (K_{++} + K_{--}) \pm \sqrt{(K_{++} - K_{--})^2 + 4|K_{+-}|^2} \right). \quad (2.36)$$

Note that the matrix  $K_{\sigma\sigma'}$  is hermitian with positive eigenvalues, as it should be. Then the orthonormalized mode functions are given by

$$\begin{aligned} v_{p\sigma lm} &= V_{p\sigma} Y_{plm}; \\ V_{p\sigma} &= \frac{1}{a(t)\sqrt{\lambda_{\sigma}}} (M_{\sigma+} \chi_p + M_{\sigma-} \chi_{-p}). \end{aligned} \quad (2.37)$$

### B. de Sitter super-curvature mode

Next we consider the discrete mode that arises due to the spacetime structure of de Sitter space. As mentioned above we consider the wall perturbation mode separately later. For convenience, we set  $p = i\Lambda$  and look for a possible value of  $\Lambda$ . When there is no bubble wall, it has been shown that there arises a mode with  $\Lambda = \nu'$  ( $\nu' = \sqrt{9/4 - m^2/H^2} - 1/2$ ) when  $\nu' > 0$  ( $m^2 < 2H^2$ ) [12]. In the present case, because the wall is present and the mass changes from  $M$  to  $m$ , such a mode may or may not exist, depending on the function  $\mathcal{M}^2$  even if  $m^2 < 2H^2$ .

In the region C, we consider the solution of the form,

$$u_{\Lambda lm}(r_C, t_C, \Omega) = \frac{1}{a_E(t_C)} \chi_{\Lambda}(t_C) \frac{P_{-\Lambda-1/2}^{-l-1/2}(i \sinh r_C)}{\sqrt{i \cosh r_C}} Y_{lm}(\Omega), \quad (2.38)$$

where we set the form of  $\chi_{\Lambda}$  as

$$\chi_{\Lambda} = \begin{cases} \alpha_{\Lambda} P_{\mu'}^{\Lambda}(\sin t_C - i0) + \beta_{\Lambda} P_{\mu'}^{-\Lambda}(\sin t_C - i0), & (t_C \rightarrow -\pi/2), \\ P_{\nu'}^{-\Lambda}(\sin t_C - i0) + \gamma_{\Lambda} P_{\nu'}^{\Lambda}(\sin t_C - i0), & (t_C \rightarrow \pi/2), \end{cases} \quad (2.39)$$

near the both boundaries of the region C. The regularity condition at  $t_C = -\pi/2$  is that the mode function should be less singular than  $(t_C + \pi/2)^{-1}$ , hence  $\chi_{\Lambda} \rightarrow 0$ . Using the asymptotic behavior of  $P_{\nu}^{\mu}(z)$  at  $z \rightarrow -1$  [25], this requires the ratio of  $\beta_{\Lambda}$  to  $\alpha_{\Lambda}$  to be

$$\beta_{\Lambda} = \frac{\sin \pi \mu'}{\pi} \Gamma(1 + \Lambda + \mu') \Gamma(\Lambda - \mu') \alpha_{\Lambda}. \quad (2.40)$$

Similarly, the regularity condition at  $t_C = \pi/2$  demands that  $\gamma_{\Lambda}$  should vanish:

$$\gamma_{\Lambda} = 0. \quad (2.41)$$

Then we need to solve the Eq. (2.18) with the above boundary conditions in both ends. Thus the problem is to find the eigenvalue  $\Lambda$  and the corresponding normalized eigenmode. This eigenvalue problem will be solved for a simple model in section 4.

Now let us consider the normalization of the super-curvature mode. The Klein-Gordon inner products of the mode functions  $u_{\Lambda lm}$  are calculated in the region C as

$$\begin{aligned} &\langle u_{\Lambda lm}(r_C, t_C, \Omega), u_{\Lambda' m'}(r_C, t_C, \Omega) \rangle \\ &= -i \cosh^2 r_C \int_{-\infty}^{\infty} d\xi a_E^2 \int d\Omega \left\{ u_{\Lambda lm} \frac{\partial \overline{u_{\Lambda' m'}}}{\partial r_C} - \frac{\partial u_{\Lambda lm}}{\partial r_C} \overline{u_{\Lambda' m'}} \right\} \\ &= \frac{2N_{\Lambda}}{\Gamma(\Lambda + l + 1)\Gamma(-\Lambda + l + 1)} \delta_{l'l'} \delta_{mm'}, \end{aligned} \quad (2.42)$$

where

$$N_{\Lambda} := \int_{-\infty}^{\infty} d\xi |\chi_{\Lambda}|^2. \quad (2.43)$$

Thus, the normalized mode functions  $v_{\Lambda lm}$  are given by

$$v_{\Lambda lm} = \sqrt{\frac{\Gamma(\Lambda + l + 1)\Gamma(-\Lambda + l + 1)}{2N_\Lambda}} u_{\Lambda lm}. \quad (2.44)$$

In particular, by analytic continuation to the region R (inside the bubble), we obtain the de Sitter super-curvature mode functions in the open universe as

$$v_{\Lambda lm}(t_R, r_R, \Omega) = \frac{1}{\sqrt{N_\Lambda}} \frac{P_1^{-\Lambda}(\cosh t_R)}{H^{-1} \sinh t_R} \mathcal{Y}_{\Lambda lm}(r_R, \Omega), \quad (2.45)$$

where

$$\mathcal{Y}_{\Lambda lm} := \sqrt{\frac{\Gamma(\Lambda + l + 1)\Gamma(-\Lambda + l + 1)}{2}} \frac{P_{\Lambda-1/2}^{-l-1/2}(\cosh r_R)}{\sqrt{\sinh r_R}} Y_{lm}(\Omega). \quad (2.46)$$

### C. Wall fluctuation mode

Recently, several authors have discussed the effect of the bubble wall fluctuations [11,14,15]. The wall fluctuation mode appears when we consider the quantum fluctuations of the tunneling field itself, which is the case of a single field model. As mentioned before,  $\mathcal{M}^2$  should be regarded as  $V''(\sigma_B)$  in this case.

Since the wall fluctuation mode is one of the discrete modes, the formula obtained in the previous subsection is applicable. However, besides the fact that the origin of the discrete spectrum is different from the de Sitter super-curvature mode, the corresponding solution of the Eq. (2.18),  $\chi_W$ , can be written down formally in this special case. Hence we consider this mode separately in this subsection.

It is well known that the time derivative of the bounce solution satisfies the equation of fluctuations, related to the zero mode problem [26]. In fact, we can derive the following equation directly from Eq. (2.10),

$$\left[ \frac{H^2}{a_E^3} \frac{d}{dt_C} a_E^3 \frac{d}{dt_C} - \frac{3}{a_E^2} - V''(\sigma_B) \right] \frac{d\sigma_B}{dt_C} = 0. \quad (2.47)$$

This is just the equation of fluctuations, i.e., eq.(2.11) with the eigenvalue of  $-\mathbf{L}^2$  given by  $1 + p^2 = -3$ , or  $\Lambda^2 = -p^2 = 4$ . Then if they have finite Klein-Gordon norms, they will contribute to the quantum fluctuations inside the bubble.

Therefore let us consider the mode functions

$$u_{W,lm} = \frac{d\sigma_B}{d(H^{-1}t_C)} \frac{P_{3/2}^{-l-1/2}(i \sinh r_C)}{\sqrt{i \cosh r_C}} Y_l^m(\Omega). \quad (2.48)$$

Calculating the Klein-Gordon norms, we obtain

$$\langle u_{W,lm}, u_{W,l'm'} \rangle = \frac{2\mathcal{N}_W}{\Gamma(l+3)\Gamma(l-1)} \delta_{ll'} \delta_{mm'}, \quad (2.49)$$

where

$$\mathcal{N}_W := H \int_{-\pi/2}^{+\pi/2} dt_C a_E \left| \frac{d\sigma_B}{dt_C} \right|^2 = \int_{-\infty}^{+\infty} d\xi \left| \frac{d\sigma_B}{d\xi} \right|^2. \quad (2.50)$$

Note that  $\mathcal{N}_W$  has the dimension of (mass)<sup>2</sup>. As one can readily see, the Klein-Gordon norms vanish for  $l = 0$  and 1. One may think that they give a divergent contribution to the fluctuations. However, they simply represent the temporal and spatial translations of the origin of the bounce solution, i.e., they are the zero modes. Hence we do not have to take these modes into account [26]. On the other hand, the modes with  $l \geq 2$  do have finite Klein-Gordon norms and they contribute to the fluctuations [11]. We note that in the exact thin-wall limit, the amplitude of these modes are non-zero only on the bubble wall and they do not contribute to the fluctuations in the open universe (region R). It is crucially important that  $\dot{\sigma}_B$  is not exactly zero off the wall, however small it may be. Then the normalized mode functions are given by

$$v_{W,lm} = \sqrt{\frac{\Gamma(l+3)\Gamma(l-1)}{2\mathcal{N}_W}} u_{W,lm}. \quad (2.51)$$



Analytically continuing the mode functions into the region R, we have in the open universe,

$$v_{W,lm}(r_R, t_R, \Omega) = \frac{1}{\sqrt{\mathcal{N}_W}} \frac{d\sigma_B}{d(H^{-1}t_R)} \mathcal{Y}_{\Lambda=2,lm}(r_R, \Omega), \quad (2.52)$$

where  $\mathcal{Y}_{\Lambda lm}$  has been defined in Eq. (2.46). An important property of this mode is that the second rank tensor constructed from the spatial harmonic function happens to be transverse-traceless [11]. Furthermore, the gauge-invariant density perturbation  $\Delta$ , which represents the density perturbation on the comoving hypersurface, vanishes identically. Thus it may be viewed as a kind of gravitational wave mode [14]. However, in order to treat all the modes on an equal footing, we do not take that view here.

To summarize this section, we have discussed the three distinct kinds of mode functions which describe quantum fluctuations in open inflation models. The first one is the usual modes having continuous spectrum. The other two are modes with discrete spectra; the de Sitter super-curvature mode and the wall fluctuation mode. These quantum fluctuations give rise to cosmological metric perturbations which will be reflected in observational quantities. We will discuss this aspect of the quantum fluctuations in the next section.

### III. INITIAL FLUCTUATIONS IN OPEN UNIVERSE AND LARGE ANGLE CMB ANISOTROPIES

Once we have the mode functions which describe the quantum state of the inflaton field inside the bubble, we can investigate the evolution of resulting cosmological perturbations in the open inflationary stage and the subsequent stage of the open Friedmann universe, which can be compared with observational data. In this section, we first consider the initial condition of the cosmological perturbations generated during the open inflationary stage, based on the results obtained in the previous section. Since the inflaton is almost massless during the open inflationary stage inside the bubble, we set  $m^2 = 0$ . Then we relate it to the spectrum of large angular scale CMB anisotropies. Below, we work in the region R which describes the open universe inside the bubble. We write the line element as

$$\begin{aligned} ds^2 &= -dt^2 + a^2(t)\gamma_{ij}dx^i dx^j \\ &= a^2(\eta) \left[ -d\eta^2 + \gamma_{ij}dx^i dx^j \right], \end{aligned} \quad (3.1)$$

where  $a$  is the scale factor,  $t$  is the cosmological proper time,<sup>‡</sup>  $\eta$  is the conformal time, and

$$\gamma_{ij}dx^i dx^j = dr^2 + \sinh^2 r d\Omega^2. \quad (3.2)$$

At the open inflationary stage, the scale factor is assumed to be given by

$$a = \frac{\sinh Ht}{H} = \frac{1}{H \sinh(-\eta)}, \quad (3.3)$$

where  $H$  is sufficiently slowly varying in time.

Just after the bubble is formed, or in the spacetime region close to the boundary light cone of the region R, the universe is dominated by the curvature term, or the matter energy density can be neglected. Hence the metric perturbations induced by the quantum fluctuations of the scalar field are negligible. On the other hand, there exists a time slicing on which the effect of metric perturbations is minimal, called the flat hypersurfaces. This implies that the fluctuations described by the mode functions we have obtained in the previous section may be regarded as those on the flat hypersurfaces. It is easy to show that the curvature perturbation on the comoving hypersurface  $\mathcal{R}_c$  is related to the scalar field perturbation  $\varphi$  on the flat hypersurface as  $\mathcal{R}_c = -\dot{a}/(a\dot{\phi}_B)\varphi$  [27]. Assuming the perturbation is adiabatic,  $\mathcal{R}_c$  completely determines the metric and matter perturbations of scalar type (i.e., those which can be expanded in terms of scalar harmonics on the 3-space). An important property of  $\mathcal{R}_c$  is that it remains constant on superhorizon scales as long as the perturbation is adiabatic, irrespective of the background spatial curvature of the universe (see Appendix A). Hence what we need to evaluate is the amplitude of  $\mathcal{R}_c$  for each mode when the mode passes the horizon scale. Assuming  $\dot{\phi}_B$  and  $H$  are sufficiently slowly varying at the inflationary stage, we may then evaluate  $\mathcal{R}_c$  at the limit  $\eta \rightarrow 0$  ( $a \rightarrow \infty$ ). Thus we have

$$\mathcal{R}_c = -\frac{H}{\dot{\phi}_B}\varphi; \quad \eta \rightarrow 0. \quad (3.4)$$

---

<sup>‡</sup>Up to now we have used the non-dimensional time normalized by the Hubble parameter. But from now on, we recover the dimension of time in  $t$ .

The spectrum of the curvature perturbation on the comoving hypersurfaces is given as follows. Expanding the curvature perturbation by modes

$$\begin{aligned} \mathcal{R}_c = & \sum_{\sigma lm} \int_0^\infty dp \mathcal{R}_{p\sigma} Y_{plm}(r, \Omega) \\ & + \sum_{lm} \mathcal{R}_\Lambda \mathcal{Y}_{\Lambda lm}(r, \Omega) + \sum_{lm} \mathcal{R}_W \mathcal{Y}_{2lm}(r, \Omega), \end{aligned} \quad (3.5)$$

the power spectrum of the curvature perturbation is given by  $|\mathcal{R}_p|^2 := \sum_\sigma |\mathcal{R}_{p\sigma}|^2$  for continuous modes, by  $|\mathcal{R}_\Lambda|^2$  for de Sitter super-curvature mode, and by  $|\mathcal{R}_W|^2$  for wall fluctuation mode.

First consider the continuous modes. From Eqs. (2.37) and (3.4), we find after some algebra,

$$|\mathcal{R}_p|^2 = \left( \frac{H^2}{\dot{\phi}_B} \right)^2 \frac{\coth \pi p}{2p(1+p^2)} (1-Y), \quad (3.6)$$

where

$$Y = \frac{\Gamma(2-ip)}{\Gamma(2+ip)} \frac{e^{-\pi p} \beta_p}{2 \cosh \pi p \alpha_p} + \text{c.c.} \quad (3.7)$$

It may be worthwhile to compare this result with the spectra of the Bunch-Davies vacuum state [5,13] and the conformal vacuum state [27,28]. In these case we have

$$|\mathcal{R}_p|_{BD}^2 = \left( \frac{H^2}{\dot{\phi}_B} \right)^2 \frac{\coth \pi p}{2p(1+p^2)}, \quad (3.8)$$

$$|\mathcal{R}_p|_C^2 = \left( \frac{H^2}{\dot{\phi}_B} \right)^2 \frac{1}{2p(1+p^2)}, \quad (3.9)$$

respectively. The result of our model (3.6) differs from that of the Bunch-Davies one in the last factor  $(1-Y)$ , which represents the effect of the mass difference outside the wall. However, as  $Y \rightarrow 0$  for  $p \rightarrow \infty$ , the spectra in all the three cases behave as  $|\mathcal{R}_p|^2 \propto 1/p^3$  for  $p \gg 1$ , which shows the perturbations have the Harrison-Zel'dovich spectrum on scales smaller than the curvature scale, irrespective of the choice of vacuum. The difference appears on and above the curvature scale, and it may become important when considering large angular scale CMB anisotropies.

As for the de Sitter super-curvature mode, the spectral amplitude is given from Eq. (2.45) as

$$|\mathcal{R}_\Lambda|^2 = \left( \frac{H^2}{\dot{\phi}_B} \right)^2 \frac{1}{N_\Lambda \Gamma(2+\Lambda)^2}. \quad (3.10)$$

We note that, in the Bunch-Davies vacuum limit, we have  $\Lambda \rightarrow 1$  and  $N_\Lambda \rightarrow 1/2$ , which gives

$$|\mathcal{R}_\Lambda|_{BD}^2 = \left( \frac{H^2}{\dot{\phi}_B} \right)^2 \frac{1}{2}. \quad (3.11)$$

The amplitude of the wall fluctuation mode is given from Eq. (2.52). We identify  $\sigma_B$  with  $\phi_B$  and note that  $d\sigma_B/dt_R = H^{-1}\dot{\sigma}_B$ . Then

$$|\mathcal{R}_W|^2 = \frac{H^2}{\mathcal{N}_W}. \quad (3.12)$$

One sees it is quite different from those of the other modes; it contains no information of how the field evolves at the open inflationary stage but is completely determined by the part of the potential which governs the false vacuum decay.

Now we consider the CMB anisotropies predicted in our open inflation models using the initial conditions obtained in the above. The power spectra of CMB anisotropies in open models have been well investigated in the case when the scalar field is in the conformal vacuum [27–30] or in the Bunch-Davies vacuum [5,13]. Since we expect the difference between the present models and the previously investigated models arises only on large angular scales, we focus on low multipoles ( $l < 20$ ) of the spectrum. Concerning the wall fluctuation mode, as we have mentioned, it has a very interesting property that the perturbation in the spatial curvature induced by it is transverse-traceless [11]. Hence it

may be regarded as a tensor mode perturbation. Garriga have investigated the evolution of this mode in the open inflationary universe from this point of view [14]. However, in this paper we treat it as a usual scalar perturbation except for the fact that  $p^2 = -4$ . For completeness, a proof that both approaches are equivalent is given in Appendix B.

From the perturbed Einstein equations, the evolution equation of  $\mathcal{R}_c$  becomes

$$\mathcal{R}_c'' + 2\frac{a'}{a}\mathcal{R}_c' - K\mathcal{R}_c = \mathcal{S}, \quad (3.13)$$

where the prime denotes the conformal time derivative,  $K = -1$  for an open universe and the source term  $\mathcal{S}$  can be neglected if the universe is matter-dominated (see Appendix A). Since  $\mathcal{R}_c = \text{const.}$  at the very early stage of the hot Friedmann universe, the relevant solution of it is the so-called growing mode solution. Here we consider  $\mathcal{R}_c$  on sufficiently large scales that it re-enters the horizon after the universe becomes matter-dominated. In this case, the line element is described by Eq. (3.1) with the scale factor  $a(\eta) \propto \cosh \eta - 1$  ( $\eta > 0$ ). Then we obtain

$$\mathcal{R}_c = \mathcal{R}_{c,i} \frac{3(\eta \sinh \eta - 2 \cosh \eta + 2)}{(\cosh \eta - 1)^2}, \quad (3.14)$$

where  $\mathcal{R}_{c,i}$  is the initial amplitude determined at the inflationary stage of the universe, the spectrum of which is given by Eqs. (3.6), (3.10) and (3.12).

Given the solution (3.14), we can compute the temperature fluctuations in the open universe in the gauge-invariant formalism [31]. For this purpose, we consider the gauge-invariant variables  $\Psi$  and  $\Phi$  which describe the gravitational potential perturbation and the curvature perturbation, respectively, on Newtonian slicing [32]. We have  $\Psi + \Phi = 0$  in the present case. Then  $\Phi$  is related to  $\mathcal{R}_c$  as (see Appendix A)

$$\Phi = \mathcal{R}_c + \frac{a'}{a}\mathcal{R}_c', \quad (3.15)$$

which gives

$$\Phi(\eta) = \mathcal{R}_{c,i}F(\eta), \quad (3.16)$$

where

$$F(\eta) = \frac{3(\sinh^2 \eta - 3\eta \sinh \eta + 4 \cosh \eta - 4)}{(\cosh \eta - 1)^3}. \quad (3.17)$$

Note that we have  $\Phi = \frac{3}{5}\mathcal{R}_c$  in the limit  $\eta \rightarrow 0$ . The potential perturbation gives rise to CMB anisotropies on large angular scales. Writing the temperature autocorrelation function in the form,

$$C(\theta) = \frac{1}{4\pi} \sum_l (2l+1) C_l P_l(\cos \theta), \quad (3.18)$$

the multipole moment  $C_l$  is given by a sum of contributions from the continuous modes and the two super-curvature modes,

$$C_l = C_l^{(C)} + C_l^{(S)} + C_l^{(W)}. \quad (3.19)$$

Assuming that the conformal time of the last scattering surface is sufficiently small,  $\eta_{LSS} \ll 1$ , but the universe is well matter-dominated by that time, we obtain [31]

$$C_l^{(C)} = \int_0^\infty dp |\mathcal{R}_p|^2 \left[ \frac{1}{3} F(\eta_{LSS}) f_{pl}(\eta_0 - \eta_{LSS}) + 2 \int_{\eta_{LSS}}^{\eta_0} \frac{dF(\eta')}{d\eta'} f_{pl}(\eta_0 - \eta') d\eta' \right]^2, \quad (3.20)$$

$$C_l^{(S)} = |\mathcal{R}_\Lambda|^2 \left[ \frac{1}{3} F(\eta_{LSS}) \tilde{f}_{\Lambda l}(\eta_0 - \eta_{LSS}) + 2 \int_{\eta_{LSS}}^{\eta_0} \frac{dF(\eta')}{d\eta'} \tilde{f}_{\Lambda l}(\eta_0 - \eta') d\eta' \right]^2, \quad (3.21)$$

$$C_l^{(W)} = |\mathcal{R}_W|^2 \left[ \frac{1}{3} F(\eta_{LSS}) \tilde{f}_{2l}(\eta_0 - \eta_{LSS}) + 2 \int_{\eta_{LSS}}^{\eta_0} \frac{dF(\eta')}{d\eta'} \tilde{f}_{2l}(\eta_0 - \eta') d\eta' \right]^2, \quad (3.22)$$

where  $\eta_0$  is the conformal time at present,  $f_{pl}$  is the function given in Eq. (2.15) and

$$\tilde{f}_{\Lambda l} = \sqrt{\frac{\Gamma(\Lambda + l + 1)\Gamma(-\Lambda + l + 1)}{2} \frac{P_{\Lambda-1/2}^{-l-1/2}(\cosh r_R)}{\sqrt{\sinh r_R}}}. \quad (3.23)$$

Here a word of caution is appropriate. The redshift of the matter-radiation equal time is  $z_{eq} \approx 4.2 \times 10^4 \Omega_0 h^2$ , where  $h$  is the Hubble constant normalized by 100 km/sec/Mpc and  $h \lesssim 1$  from observations. In addition,  $\cosh \eta_{LSS} = 1 + (\Omega_0^{-1} - 1)/(1 + z_{LSS})$  where  $z_{LSS}$  is the redshift of the last scattering surface ( $\sim 1000$ ). Therefore the above formula for  $C_l$  becomes inaccurate for  $\Omega_0 \ll 0.1$ . We should also note that we have put  $\eta_{LSS} = 0$  for simplicity in actual calculations. Hence our results presented in the next section may have errors of  $\sim 10\%$  for  $\Omega_0 \sim 0.1$ .

Before closing this section, we mention that the formalism developed in the previous two sections can be extended to more general cases. Namely, as long as the regions R and L are described by de Sitter space, it is not necessary to have the same Hubble parameter for these two regions. Let  $H_R$  and  $H_L$  denote the Hubble parameters in the region R and L, respectively. Then it is easily recognized that all  $H$ 's appearing in the formulas in the present section should be identified with  $H_R$ . Further, in this case, as the scale factor is different from that of de Sitter space in the region C, but the formulas written in terms of the conformal coordinate  $\xi$  do not contain  $H$  explicitly except for Eq. (2.18), what we need to do is to replace the potential in Eq. (2.18) by

$$U(\xi) \rightarrow \frac{1}{a_E} \frac{d^2 a_E}{d\xi^2} - 1 + a_E^2 \mathcal{M}^2, \quad (3.24)$$

where  $\xi$  is now defined in such a way that the metric in the region C takes the form (2.17) with  $a_E(\xi)$  being a general function of  $\xi$ .

#### IV. SPECTRUM OF THE CMB ANISOTROPIES PREDICTED BY SOME MODELS

In this section, we apply our formulas obtained in sections 2 and 3 to simple models of the open inflation scenario.

##### A. Single field model

We first consider a model with a single scalar field with the potential as shown in Fig. 1(a). The tunneling field becomes the inflaton field after the tunneling. Thus the mass square of the fluctuation field  $\varphi$  is given by  $\mathcal{M}^2(\tau) = V''(\sigma_B)$ . Its typical shape is rather complicated as shown in Fig. 3.

Because of the complexity of  $\mathcal{M}^2(\tau)$ , the analysis of this model is difficult in general. However, the mass of the inflaton in the false vacuum  $M$  must be large compared with  $H$  in order that the tunneling is not dominated by the Hawking-Moss instanton [33] as explained in Ref. [7]. Furthermore, as there are many subtleties<sup>§</sup> in models with  $M^2 \sim H^2$ , we leave it as a future problem. Here we assume  $M^2 \gg H^2$ .

Then the potential barrier between the two asymptotic regions at  $\xi \rightarrow \pm\infty$  is so high that the coherence between regions R and L are exponentially suppressed as long as we consider the modes with  $p^2 \ll M^2/H^2$ , which is the case of our present interest. So one of the two modes corresponding to the same  $p$  can be set to vanish at  $\xi \rightarrow -\infty$  and the other at  $\xi \rightarrow +\infty$ . Then automatically they are orthogonal to each other. Since the field equation (2.18) is real in the region C, we can choose the mode which vanish in the region L to be real in the region C. Then analytically continuing it to the region R, the normalized mode which does not vanish in the region R can be written as

$$V_p^{(R)} = \begin{cases} \frac{\sqrt{\pi}}{2a(t_R) \sinh \pi p} \left( e^{\pi p/2 + i\delta_p} (z_R - ip) \left( \frac{z_R + 1}{z_R - 1} \right)^{ip} + e^{-\pi p/2 - i\delta_p} (z_R + ip) \left( \frac{z_R + 1}{z_R - 1} \right)^{-ip} \right), & (\text{in R}) \\ 0, & (\text{in L}) \end{cases}, \quad (4.1)$$

where we set  $m = 0$  and  $\delta_p$  is a real constant which depends on the detail of the potential. Using this mode function, the amplitude of  $\mathcal{R}_p$  is evaluated as

$$|\mathcal{R}_p|^2 = \left( \frac{H^2}{\dot{\sigma}_B} \right)^2 \frac{\cosh \pi p + \cos 2\delta_p}{2p(1 + p^2) \sinh \pi p}. \quad (4.2)$$

---

<sup>§</sup> For example, the formalism developed in [17] which we used as a given result in the present paper is not applicable to the case in which the wall is spreading so broadly that we cannot approximate  $\sigma_B(\tau)$  by  $\sigma_F$  for  $\tau < 0$ . When  $M^2 \sim H^2$ , the wall necessarily becomes broad.

Comparing this result with the spectra for the Bunch-Davies vacuum (3.8) and the conformal vacuum (3.9), we find that the difference between the present spectrum and  $|\mathcal{R}_p|_{BD}^2$  is no more greater than the difference between  $|\mathcal{R}_p|_{BD}^2$  and  $|\mathcal{R}_p|_C^2$ . As was clarified in [5], the effect of the difference between the Bunch-Davies vacuum and the conformal vacuum on  $C_\ell^{(C)}$  is always negligibly small independent of  $\Omega_0$ . Thus as far as the continuous modes are concerned, we do not have to perform further calculations.

Next we consider the discrete mode. As mentioned above, the wall fluctuation mode is always present when we consider the fluctuations of the tunneling field itself. Then the question is whether there exists another discrete mode like the de Sitter super-curvature mode. The answer is no as long as  $M^2 \gg H^2$ . The reason why is explained in the Appendix C. In the general case, we do not have an answer to this question,\*\* but we do not discuss the de Sitter super-curvature mode any further. We focus on the wall fluctuation mode below.

The wall thickness is roughly evaluated by the inverse of the curvature scale of the potential as  $M^{-1}$ . Since we are now assuming that  $M^2 \gg H^2$ , it will not be too crude to adopt the thin-wall approximation. Then one can evaluate  $\mathcal{N}_W$  as

$$\begin{aligned}\mathcal{N}_W &= H \int d\tau a_E(\tau) \left(\frac{d\sigma_B}{d\tau}\right)^2 \approx RS_1; \\ S_1 &:= H \int d\tau \left(\frac{d\sigma_B}{d\tau}\right)^2,\end{aligned}\tag{4.3}$$

where  $S_1$  is the tension of the wall. If one uses the reduced Euclidean action written in terms of  $R$ ,  $S_1$ , and the potential energy density inside the bubble  $V_R$  (true vacuum) and outside the bubble  $V_L$  (false vacuum),  $R$  is determined in terms of the other parameters by minimizing the action as [37,15]

$$R = \frac{3S_1}{\sqrt{(\Delta V + 6\pi GS_1^2)^2 + 24\pi GV_R S_1^2}},\tag{4.4}$$

where  $\Delta V = V_L - V_R$ . Then the final result for the amplitude of the wall fluctuation mode is

$$\begin{aligned}|\mathcal{R}_W|^2 &= \frac{8\pi GV_R}{9S_1^2} \sqrt{(\Delta V + 6\pi GS_1^2)^2 + 24\pi GV_R S_1^2} \\ &= \frac{H_R^2}{8\pi GS_1^2} \sqrt{(H_L^2 - H_R^2 + (4\pi GS_1)^2)^2 + (8\pi GS_1 H_R)^2},\end{aligned}\tag{4.5}$$

where  $H_L$  and  $H_R$  are the Hubble parameters in the regions L and R, respectively. Note that although we assumed  $(H_L - H_R)/H_R \ll 1$ , the difference  $H_L - H_R$  may not be negligible in the determination of the amplitude of the wall fluctuation mode.

Now we consider the CMB power spectrum due to the wall fluctuation mode. Fig. 4 shows the power spectrum of CMB anisotropies  $l(l+1)C_l^{(W)}$  for various values of  $\Omega_0$ . The curves are normalized by  $H^2/RS_1$ . As discussed before, the amplitude of the CMB anisotropies due to the wall fluctuation mode are determined by the nature of the bubble wall. This gives an independent constraint on open inflation models. In particular, the spectrum of CMB anisotropies rises sharply towards lower multipoles for open models with  $\Omega_0 \gtrsim 0.2$ . Hence if this mode dominates over the other mode contributions, such single field models will be severely excluded by the COBE data [38]. This issue has been recently investigated by Garriga [14] and Garcia-Bellido [15].

To carry on a further analysis, we have to specify the model in more details. Let us parametrize the potential  $V(\sigma)$  by  $M^2$ ,  $V_L$ ,  $V_b$  and  $\Delta V$  as shown in Fig. 1(a). We assume  $V(\sigma) \ll M_{pl}^4$ ,  $M \ll M_{pl}$  where  $M_{pl}$  is the Planck mass,  $\Delta V/V_L \ll 1$  and the potential has the unique curvature scale  $M^2$  in the region C. Then, as the wall thickness is essentially given by  $M^{-1}$ , we have

$$S_1 \sim \frac{V_b}{M}.\tag{4.6}$$

Further we assume  $V(\sigma) \sim \lambda M_{pl}^4 (\sigma/M_{pl})^{2n}$  ( $n = 1, 2, \dots$ ) on the right of the barrier, where  $\lambda \ll 1$  as in the chaotic inflation.

---

\*\*We note an issue related to this problem. One can show that the non-existence of another discrete mode in the range  $-4 < p^2 < 0$  is a sufficient condition for the uniqueness of the negative eigenvalue mode in the one-loop order calculation of the tunneling rate in the path integral approach [34–36]. But the uniqueness has not been proved for the tunneling on the de Sitter background as far as we know.

There are three requirements to be satisfied. 1) The tunneling must be dominated not by the Hawking-Moss instanton but by the Coleman-De Luccia instanton. This requires that  $M^2 > 4H^2$ . 2) The tunneling rate  $\Gamma$  must be suppressed enough in order to avoid the fluctuations caused by the bubble collisions. This implies that [8,9]

$$-\ln(\Gamma/H^4) \sim \frac{27\pi^2 S_1^4}{2\Delta V^3} \gg 1. \quad (4.7)$$

3) Finally, the wall fluctuation mode must not dominate  $\mathcal{R}_c$ . Noting that the contribution of the continuous modes to its power in the logarithmic interval of  $p$  at  $p \gg 1$  is  $\langle \mathcal{R}_c^2 \rangle := \lim_{p \rightarrow \infty} |\mathcal{R}_p|^2 p^3 / (2\pi^2)$ , this requires

$$|\mathcal{R}_W|^2 \lesssim \langle \mathcal{R}_c^2 \rangle = \left( \frac{H_R^2}{2\pi\dot{\sigma}_B} \right)^2. \quad (4.8)$$

We assume the requirement 1) is satisfied and investigate the conditions on the potential parameters derived from the requirements 2) and 3).

From the slow roll equation of motion, we have  $|H_R^2/\dot{\sigma}_B| = 8\pi H_R V_R / |V'(\sigma_B)| = 8\pi\zeta H_R / M_{pl}$ , where  $\zeta \gtrsim 1$ . Therefore

$$\frac{|\mathcal{R}_W|^2}{\langle \mathcal{R}_c^2 \rangle} = \frac{\pi}{8\zeta^2} \sqrt{\left(1 + \frac{\Delta V}{6\pi G S_1^2}\right)^2 + \left(\frac{H_R}{2\pi G S_1}\right)^2}. \quad (4.9)$$

Since the left hand side of this must be smaller than unity, we should have

$$\frac{\Delta V}{6\pi G S_1^2} \lesssim \zeta^2 \quad \text{and} \quad \frac{H_R}{2\pi G S_1} \lesssim \zeta^2. \quad (4.10)$$

Using the fact  $S_1 \sim V_b/M$  and  $\Delta V \ll V_L$ , we find the first inequality is automatically satisfied if the second one is, which is re-expressed as

$$\frac{V_b}{V_L} \gtrsim \frac{H_R M M_{pl}^2}{2\pi\zeta^2 V_L} = \frac{4}{3\zeta^2} \left( \frac{H_R}{H_L} \right) \frac{M}{H_L}. \quad (4.11)$$

If this condition is satisfied, we also find the requirement 2) is fulfilled. Thus if the potential barrier is high enough, approximately of  $O(M/H_L) \times V_L$ , the wall fluctuation mode will become harmless. Apart from the intrinsic unnaturalness of a single field model, it is not difficult to construct models which satisfy the above constraint. Hence we conclude that a single field model remains still viable.

## B. Two-field model

Next we consider a two-field model in which the tunneling field  $\sigma$  and the inflaton in the nucleated bubble  $\phi$  are different. The supernatural inflation model proposed by Linde and Mezhlumian [7] is included in this category. We consider the following situation. Before tunneling,  $\phi$  is at the minimum of the potential  $\phi_L$  with mass  $M$ . During the tunneling, the potential of  $\phi$  changes to an almost flat but slightly declined one, i.e.,  $V'_\phi \neq 0$  and  $V''_\phi \sim 0$ . Thus  $\phi_L$  is no longer the minimum of the potential in the nucleated bubble. Therefore  $\phi$  begins the slow rolling to the new minimum of the potential.

In the following calculation, we assume that the gradient of the potential is so small that we can neglect its effect in estimating the amplitude of the fluctuations  $\varphi$ , though the condition under which this neglect is justified is not clear. Then our present formalism can be applied. For simplicity, we also assume that the thin wall approximation is valid. We denote the radius of bubble wall by  $R = a_E(\tau_0) = H^{-1} \cos \tau_0$ . Then the bubble wall trajectory in the Lorentzian region is described by the hypersurface  $t_C = \tau_0 = \text{const.}$  in the region C.

Under these assumptions, we can evaluate the fluctuation spectrum inside the bubble by applying the formulas obtained in section 3 with  $\mathcal{M}^2$  given by

$$\mathcal{M}^2 = \begin{cases} 0; & (\tau_0 < t_C < \pi/2), \\ M^2; & (-\pi/2 < t_C < \tau_0). \end{cases} \quad (4.12)$$

The form of the potential  $U(\xi)$  in Eq. (2.18) in this case is illustrated in Fig. 5. Thus the parameters of the present open inflationary model are the mass of the inflaton field in the false vacuum  $M$ , the wall radius  $R$  and the Hubble parameter  $H$ .

First we consider the continuous spectrum. As the mass is constant both outside and inside the wall, we find that the solution of the Eq. (2.18) becomes

$$\begin{aligned}\chi_p^{(R)}(t_C) &= P_{\nu'}^{ip}(\sin t_C - i0); & (\tau_0 < t_C < \pi/2) \\ \chi_p^{(L)}(t_L) &= P_{\mu'}^{ip}(\sin t_C - i0); & (-\pi/2 < t_C < \tau_0).\end{aligned}\quad (4.13)$$

The coefficients  $\alpha_p$  and  $\beta_p$  are determined by the junction condition at the wall in the region C:

$$\begin{pmatrix} \chi_p^{(R)} \\ \frac{d\chi_p^{(R)}}{d\xi} \end{pmatrix} = \begin{pmatrix} \chi_{-p}^{(L)} & \chi_p^{(L)} \\ \frac{d\chi_{-p}^{(L)}}{d\xi} & \frac{d\chi_p^{(L)}}{d\xi} \end{pmatrix} \begin{pmatrix} \alpha_p \\ \beta_p \end{pmatrix}.\quad (4.14)$$

Then  $\alpha_p$  and  $\beta_p$  given by Eqs. (2.28) can be now easily evaluated on the wall.

We have numerically evaluated the spectrum of the continuous modes. Figs. 6 show the power spectra of  $|\mathcal{R}_p|^2$  for various values of  $M$  and  $R$ , normalized by the Bunch-Davies vacuum spectrum. Fig. 6(a) shows the case when the mass outside the bubble is  $M/H = 2$ . The lines are the power spectra for the wall radii  $HR = 0.1, 0.5, 0.7$ , and  $0.9$ . One sees the spectra for all the wall radii are almost the same and they coincide with that of the Bunch-Davies vacuum except for the small range of very small  $p$ . On the other hand, Fig. 6(b) is the case  $M/H = 10$  with the lines showing the power spectra for  $HR = 0.1, 0.5, 0.7$ , and  $0.9$ . For  $M/H \gg 1$ , we can apply the discussion given in section 4A, around Eq. (4.2). There we have seen that the spectrum does not differ much from the case of the Bunch-Davies vacuum. Thus the increase in the amplitude at  $p \lesssim 1$  will saturate as  $M/H \rightarrow \infty$ . In both Figs. 6(a) and (b), all the lines rapidly approaches unity at  $p \gg 1$ , which corresponds to the Harrison-Zel'dovich spectrum, in accordance with our expectation.

Next we turn to the discrete spectrum. Again the mode function is readily solved by means of the associated Legendre function. Thus eigenvalue problem reduces to Eq. (2.40) with  $\alpha_\Lambda$  and  $\beta_\Lambda$  given in terms of the junction condition at  $t_C = \tau_0$  as

$$\alpha_\Lambda = \frac{((P_{\mu'}^{-\Lambda}, P_{\nu'}^{-\Lambda}))}{((P_{\mu'}^{-\Lambda}, P_{\mu'}^{\Lambda}))} \Big|_{t_C=\tau_0}, \quad \beta_\Lambda = \frac{((P_{\nu'}^{-\Lambda}, P_{\mu'}^{\Lambda}))}{((P_{\mu'}^{-\Lambda}, P_{\mu'}^{\Lambda}))} \Big|_{t_C=\tau_0}.\quad (4.15)$$

It is instructive to show an analytically solvable example of this eigenvalue problem. Let us consider the case  $M^2 = 2H^2$  ( $\mu' = 0$ ) and  $m^2 = 0$  ( $\nu' = 1$ ). In this case, the associated Legendre functions are expressed in terms of elementary functions.

$$\begin{aligned}P_0^{\pm\Lambda}(z) &= \frac{1}{\Gamma(1 \mp \Lambda)} \left( \frac{z+1}{z-1} \right)^{\pm\Lambda/2}, \\ P_1^{\pm\Lambda}(z) &= \frac{z \mp \Lambda}{\Gamma(2 \mp \Lambda)} \left( \frac{z+1}{z-1} \right)^{\pm\Lambda/2},\end{aligned}\quad (4.16)$$

Also, Eq. (2.40) reduces simply to  $\beta_\Lambda = 0$ , hence from Eq. (4.15),

$$((P_1^{-\Lambda}, P_0^{\Lambda})) = 0.\quad (4.17)$$

This is easily solved to give

$$\Lambda = \frac{-x_0 + \sqrt{2 - x_0^2}}{2},\quad (4.18)$$

where  $x_0 = \sin \tau_0 = \sqrt{1 - (HR)^2}$ . This result shows that  $\Lambda$  becomes larger as the wall radius increases.

For general  $M^2$ , we need numerical evaluation. Since  $0 < \Lambda \leq 1$  in the exact de Sitter case with the upper limit attained when  $m^2 \rightarrow 0$ , we expect any introduction of finite mass outside the wall will reduce  $\Lambda$  to a value less than unity. Hence we look for an eigenvalue in the range  $0 < \Lambda < 1$ . Fig. 7 shows  $\Lambda$  as a function of  $HR$  for several values of  $M^2$  when  $m^2 = 0$ . One sees  $\Lambda$  becomes smaller as  $M^2$  becomes larger or as the wall radius becomes smaller. But the de Sitter super-curvature mode exists for any wall radius as long as  $M^2 < 2H^2$ . On the other hand, for  $M^2 > 2H^2$ , the de Sitter super-curvature mode ceases to exist when the wall radius becomes smaller than a critical value. Fig. 8 shows the critical line on the  $(M/H, HR)$ -plane on which the super-curvature mode disappears. The de Sitter super-curvature mode exists below the line.

This property of the super-curvature mode can be understood in analogy with the quantum mechanics described before. As the wall radius decreases, the position of the bubble wall  $\xi_0$  moves right in Fig. 5 of the potential  $U(\xi)$ . Also, as the mass  $M$  increases, the potential barrier outside the bubble wall  $\xi < \xi_0$  becomes higher. These make it difficult to form a bound state. We note that  $U(\xi)$  has the deepest valley when the mass  $M$  is zero. This situation corresponds to the case when we assume the Bunch-Davies vacuum state inside the bubble and when the super-curvature mode contributes extremely [5].

Now we show the results of numerical calculations of the CMB anisotropy power spectrum  $l(l+1)C_l$  in Fig. 9 for the  $\Omega_0 = 0.1$  universe with  $M^2/H^2 = 2$  and the wall radii  $HR = 0.3, 0.5, 0.7,$  and  $0.9$ . The curves are normalized by  $(3H^2/5\dot{\phi}_B)^2$ . Here both continuous and discrete modes are included. To compare the results with the previous ones [27–30,5,13], we plotted two dashed lines in the figure. The top dashed curve is the result when the scalar field is in the Bunch-Davies vacuum [5,13], and the bottom dashed curve is the one in the conformal vacuum [27–30]. All of the curves lie between these two curves. We see the amplitude becomes large as the wall radius increases, approaching that in the case of the Bunch-Davies vacuum. As described before, the contribution of the super-curvature mode is most for the Bunch-Davies vacuum and is least for the conformal vacuum. When the wall radius becomes large and the mass becomes small, the contribution from the super-curvature mode becomes large, which explains the behavior of the CMB power spectra in Fig. 9. We have also calculated the CMB spectra for the  $\Omega_0 = 0.3$  universe. The results have turned out to be almost independent of the model parameters. In fact, if only  $C_l^{(C)}$  is taken into account, the difference between the Bunch-Davies vacuum and the conformal vacuum is only a few percent even for  $\Omega_0 = 0.1$  [5]. Thus the differences are dominantly due to the de Sitter super-curvature mode  $C_l^{(S)}$ , but its contribution rapidly becomes negligible as one increases  $\Omega_0$ .

## V. CONCLUSION

We have investigated in detail the quantum fluctuations and the resultant CMB anisotropies in two simple models of one-bubble open inflationary scenario. Before going into the analysis of the specific models, we have extended the previously developed formalism to investigate the quantum state inside the nucleated bubble, and derived formulas for the mode functions which take account of the effect of the tunneling described by the Coleman-De Luccia instanton. In the main stream, we have assumed the potential energy difference between the false and true vacua is small enough so that spacetime both inside and outside the bubble can be described by de Sitter space with a single Hubble parameter  $H$ , but the results can be easily extended to more general cases.

A complete description of a quantum state requires a complete set of mode functions which are normalizable on a Cauchy surface of the whole spacetime. This brings about new sets of fluctuation modes which had not been considered in most of the previous analyses of an open inflationary universe. In addition to the usual modes with continuous spectrum, there are modes with discrete spectrum corresponding to the fluctuations on super-curvature scales. For both the continuous and discrete modes, we have obtained general formulas of the spectrum of the CMB anisotropies on large angular scales which result from the quantum fluctuations.

After these preparations, we have considered two simple classes of one-bubble open inflationary models. One is a single field model with the potential as illustrated in Fig. 1(a), assuming that the mass square in the false vacuum,  $M^2$ , is much larger than  $H^2$ . The other is a two-field model in which the false vacuum decay is mediated by a scalar field different from the inflaton inside the bubble and the inflaton is massive in the false vacuum through the coupling with the tunneling field.

In the case of a single field model with  $M^2 \gg H^2$ , there is one discrete mode which represents fluctuations of the bubble wall. We have shown that there is no other discrete mode in this model. Thus we have considered the CMB anisotropies due to the continuous modes and the wall fluctuation mode. As far as the contribution of the continuous modes to the CMB anisotropies is concerned, we have found that it is approximately the same as in the case of the Bunch-Davies vacuum or the conformal vacuum. Hence we have focused on the wall fluctuation mode. The curvature perturbation due to the wall fluctuation mode is notable. It is always present in this model and its amplitude is totally determined by the part of the potential which governs the tunneling but has nothing to do with the scalar field dynamics inside the nucleated bubble. Since its amplitude is independent of the amplitude of the curvature perturbation due to the continuous modes, its contribution to the CMB anisotropies gives rise to an independent constraint on the model, just as the gravitational wave perturbation does to the usual inflation models. Fortunately, the constraint turns out to be relatively weak. Thus it is possible to construct a model in which the effect of the wall fluctuation mode can be neglected.

Here we make the following remark. The wall fluctuation mode has a peculiar property that curvature perturbations induced by it are transverse-traceless, hence it can be regarded as a mode of tensor-type perturbations. This means that the perturbation of the scalar field might couple with the gravitational wave perturbation for this mode when the degrees of freedom of gravity are fully taken into account. But we have not incorporated them in the present analysis. Thus there remains a possibility that the final answer changes qualitatively. We hope to come back to this issue in near future.

As for a two-field model, we have adopted the thin-wall approximation and assumed the mass of the inflaton changes like the step function across the wall. Thus the model can be parametrized by the mass in the false vacuum  $M$ , the Hubble radius  $H$  and the wall radius  $R$ . In this model, the origin of the discrete mode is different from that in the single field model. Since it originates from the spacetime structure of de Sitter space, we have called it the de Sitter



super-curvature mode. The existence of the de Sitter super-curvature mode depends on the mass  $M$  of the inflaton at the false vacuum and on the radius  $R$  of the bubble wall. It appears when  $HR$  is large and  $M/H$  is small. For models with  $M/H \gg 1$ , the super-curvature mode disappears. Different from the wall fluctuation mode which appeared in the single field model, the amplitude of spatial curvature perturbations induced by this mode is determined by the scalar field dynamics at the open inflationary stage inside the bubble, as in the case of the continuous modes.

We have then investigated the spectrum of CMB anisotropies on large angular scales in this model. Though the spectra of the curvature perturbations due to the continuous modes have different shapes on the curvature scale for different model parameters, we have found the resulting CMB power spectra do not significantly depend on the parameters for  $\Omega_0 \gtrsim 0.1$ . On the other hand, the parameter-dependence appears clearly in the contribution of the de Sitter super-curvature mode to the CMB spectrum. The effect of this mode is appreciable when the wall radius is large ( $HR \sim 1$ ) and the mass is small ( $M/H \ll 1$ ). The effect is to raise the amplitudes of low multipoles at  $l \lesssim 10$  for models with  $\Omega_0 \lesssim 0.1$ . If this mode contributes significantly, the predicted CMB power spectra will contradict with COBE observations [13]. However, for an open universe of  $\Omega_0 \gtrsim 0.3$  as well as for models with small  $HR$  and large  $M/H$ , the effect of the super-curvature mode on the CMB anisotropies is practically negligible.

We comment on implications of our results to the large scale structure formation. As all our open models predict the Harrison-Zel'dovich spectrum on small scales, the difference can appear only from the normalization of the density perturbations. However, the difference will be negligible if we adopt the normalization scheme in terms of the likelihood analysis using the COBE result [38]. This is because all the models predict practically the same CMB power spectrum at  $l \gtrsim 10$ .

In summary, we have presented a detailed analysis of the quantum fluctuations in open universe in simple models of the one-bubble inflationary scenario and the resulting CMB anisotropies on large angular scales. We have found there exist ranges of model parameters which are consistent with CMB observations. Thus the one-bubble inflationary scenario is a viable one for explaining the large scale structure of the universe and it certainly deserves further study. There are of course many issues left to be clarified in future. For example, consideration of the continuous gravitational wave modes is definitely necessary. Analyses of more sophisticated models, like several other two-field models proposed by Linde and Mezhlumian [6,7] are of particular interest. Inclusion of the degrees of freedom of the gravitational perturbation in the formalism from the beginning is a difficult issue but should be done in order to gain a more firm picture of the false vacuum decay and the subsequent evolution of the quantum state.

### Acknowledgements

We thank N. Sugiyama and H. Ishihara for discussions. We also thank J. Garcia-Bellido for showing us his result prior to publication.

### APPENDIX A: DERIVATION OF THE EVOLUTION EQUATION FOR $\mathcal{R}_C$

Here we derive the evolution equation for  $\mathcal{R}_c$ . We follow the notation of Ref. [32] for the perturbation variables. Consider the general scalar harmonics on 3-space with curvature constant  $K$ , which satisfy

$$(\Delta + k^2)Y = 0. \quad (\text{A1})$$

The corresponding vector and tensor harmonics are defined as

$$Y_i = -\frac{1}{k}Y_{|i}, \quad Y_{ij} = \frac{1}{k^2}Y_{|ij} + \frac{1}{3}\gamma_{ij}Y, \quad (\text{A2})$$

where the vertical bar denotes the covariant derivative with respect to the 3-metric  $\gamma_{ij}$ . In the notation of the present paper, we have set  $K = -1$  and  $k^2 = p^2 + 1$ . But since we do not have to fix  $K$  in the discussion below, we leave it arbitrary and use  $k$  to denote the eigenvalue. Also we suppress the eigenvalue index  $k$  for notational simplicity. We expand all the perturbation variables in terms of these harmonics. Specifically, the metric is expressed as

$$ds^2 = a^2 [-(1 + 2AY)d\eta^2 - 2BY_i dx^i d\eta + ((1 + 2H_L)\gamma_{ij} + 2H_T Y_{ij}) dx^i dx^j], \quad (\text{A3})$$

and the energy-momentum tensor is expressed as

$$\begin{aligned} T^0_0 &= -\rho(1 + \delta Y), & T^i_0 &= -(\rho + p)vY^i, \\ T^i_j &= p((1 + \pi_L Y)\delta^i_j + \pi_T Y^i_j). \end{aligned} \quad (\text{A4})$$

The background equations are

$$\left(\frac{a'}{a}\right)^2 + K = \frac{8\pi G}{3}\rho a^2, \quad \rho' + 3\frac{a'}{a}(\rho + p) = 0, \quad (\text{A5})$$

where the prime denotes the derivative with respect to  $\eta$ . Then the Einstein equations for scalar-type perturbations are written as

$$\begin{aligned} \delta G^0_0 &= -8\pi G\rho\delta Y, \\ \delta G^0_i &= 8\pi G(\rho + p)(v - B)Y_i, \\ \delta G^i_j &= 8\pi G(p\pi_L Y\gamma_{ij} + p\pi_T Y_{ij}), \end{aligned} \quad (\text{A6})$$

where the explicit expressions for  $\delta G^\mu_\nu$  can be found in Appendix D of Ref. [32].

For our discussion, we need the  $(0, i)$ -component and the traceless part of  $(i, j)$ -component of the above equations. They give, respectively,

$$k\frac{a'}{a}A - k\mathcal{R}' + K\sigma_g = 4\pi G(\rho + p)a^2(v - B), \quad (\text{A7})$$

$$k^2(A + \mathcal{R}) - \frac{1}{a^2}(a^2k\sigma_g)' = -8\pi Gpa^2\pi_T, \quad (\text{A8})$$

where  $\mathcal{R} = H_L + \frac{1}{3}H_T$  and  $\sigma_g = k^{-1}H'_T - B$ . Expressing Eq. (A7) on the Newtonian hypersurface (defined by  $\sigma_g = 0$ ), for which we have  $A = \Psi$ ,  $\mathcal{R} = \Phi$ ,  $v - B = V$ , we find

$$\Phi' = \frac{a'}{a}\Psi - 4\pi G(\rho + p)a^2\frac{V}{k}. \quad (\text{A9})$$

Also, from Eq. (A8), we obtain

$$\Psi + \Phi = -8\pi G\frac{a^2}{k^2}p\Pi, \quad (\text{A10})$$

where  $\Pi = \pi_T$  is the gauge-invariant anisotropic stress perturbation.

Using the contracted Bianchi identities, which give the energy-momentum conservation law  $T_{\mu\nu}{}^{;\nu} = 0$ , one obtains the equations for the matter variables. Here we only need the  $\mu = i$  component of it, i.e., the equation for  $V$ . It is given by Eq. (4.7b)' in Chapter II of [32], which is

$$\frac{1}{a}\left(\frac{aV}{k}\right)' = \Psi + S; \quad S := \frac{c_s^2\Delta + \Gamma}{1+w} - \frac{2k^2 - 3K}{3}\frac{w}{k^2}\frac{w}{1+w}\Pi, \quad (\text{A11})$$

where  $c_s^2 = p'/\rho'$ ,  $w = p/\rho$ ,  $\Gamma$  is the gauge-invariant entropy perturbation, and  $\Delta$  is the density perturbation on the comoving hypersurface which is related to that on the Newtonian hypersurface  $\Delta_s$  as

$$\Delta = \Delta_s + 3(1+w)\frac{a'}{a}\frac{V}{k}. \quad (\text{A12})$$

Now from the gauge transformation property of  $\mathcal{R}$ , the curvature perturbation  $\mathcal{R}_c$  on the comoving hypersurface (defined by  $v - B = 0$ ) is expressed in terms of  $\Phi$  and  $V$  as

$$\mathcal{R}_c = \Phi - \frac{a'}{a}\frac{V}{k}. \quad (\text{A13})$$

Then from Eqs. (A9) and (A11), we find

$$\mathcal{R}'_c = -K\frac{V}{k} - \frac{a'}{a}S. \quad (\text{A14})$$

Taking the derivative of this equation and using Eqs. (A10) and (A11), we finally obtain

$$\mathcal{R}''_c + 2\frac{a'}{a}\mathcal{R}'_c - K\mathcal{R}_c = -\left(2\left(\frac{a'}{a}\right)^2 + K\right)S - \left(\frac{a'}{a}S\right)' + \frac{K}{k^2}8\pi Gpa^2\Pi. \quad (\text{A15})$$

We find the right hand side of this equation vanishes if the universe is matter-dominated ( $p = c_s^2 = 0$ ). Furthermore, it is known that  $\Delta = O((ka/a')^2)$  on superhorizon scales [32]. From this fact, one can easily deduce  $\mathcal{R}_c$  remains constant on super-horizon scales if  $\Gamma = \Pi = 0$ . We also note that from Eqs. (A13) and (A14),  $\Phi$  can be expressed as

$$\Phi = \mathcal{R}_c - \frac{1}{K} \frac{a'}{a} (\mathcal{R}'_c + \frac{a'}{a} S). \quad (\text{A16})$$

In particular, if  $S = 0$  as in the case of a matter-dominated universe, we have

$$\Phi = \mathcal{R}_c - \frac{1}{K} \frac{a'}{a} \mathcal{R}'_c. \quad (\text{A17})$$

With  $K = -1$ , this is the relation we have used in the text.

## APPENDIX B: EQUIVALENCE OF TENSOR AND SCALAR TREATMENTS FOR $P^2 = -4$

Here we show that the wall fluctuation mode can be treated either as a tensor-type perturbation or a scalar-type perturbation and prove the equivalence of the CMB anisotropy formulae in both approaches.

In general, setting  $\delta T/T = \Theta$ , the perturbed collisionless Boltzmann equation is written as

$$\frac{D}{d\lambda} \Theta = kA Y_i \gamma^i - (\mathcal{R}' - \frac{1}{3} k\sigma_g) Y - k\sigma_g Y_{ij} \gamma^i \gamma^j, \quad (\text{B1})$$

where  $D/d\lambda$  denotes the Lagrange derivative along the light ray with  $\lambda$  being the conformal affine parameter, and  $\gamma_i$  is the directional cosine of the photon propagation vector. Assuming the universe is matter-dominated, one has  $A = 0$  on the comoving hypersurface  $v - B = 0$ . Also, expressing Eq. (A7) on the comoving hypersurface, one obtains

$$\mathcal{R}'_c = \frac{K}{k^2} (k\sigma_g)_c, \quad (\text{B2})$$

where  $(k\sigma_g)_c$  is  $k\sigma_g$  evaluated on the comoving hypersurface. Using these facts, Eq. (B1) on the comoving hypersurface becomes

$$\frac{D}{d\lambda} \Theta_c = \frac{k^2 - 3K}{3k^2} (k\sigma_g)_c Y - (k\sigma_g)_c Y_{ij} \gamma^i \gamma^j. \quad (\text{B3})$$

In particular, for  $k^2 = 3K$  which corresponds to  $p^2 = k^2 - 1 = -4$  for  $K = -1$ , one has

$$\frac{D}{d\lambda} \Theta_c = -(k\sigma_g)_c Y_{ij} \gamma^i \gamma^j = -3\mathcal{R}'_c Y_{ij} \gamma^i \gamma^j. \quad (\text{B4})$$

Noting that  $Y_{ij}$  in this case is transverse-traceless [11], we see this is equivalent to the tensor-type perturbation with the metric perturbation  $H_{ij} = 6\mathcal{R}'_c Y_{ij}$ .

Now we go to the Newtonian slicing, in which  $\sigma_g = 0$ , by the transformation  $\eta \rightarrow \eta + T$ . Then the gauge function  $T$  is determined from

$$0 = (k\sigma_g)_c - k^2 T, \quad (\text{B5})$$

which gives

$$T = \frac{(k\sigma_g)_c}{k^2} = \frac{\mathcal{R}'_c}{K}. \quad (\text{B6})$$

Let  $\Theta_s$  denotes the temperature anisotropy on the Newtonian hypersurface. The gauge transformation affects only the monopole and dipole parts of the anisotropy. Then one finds  $\Theta_s$  is related to  $\Theta_c$  as

$$\Theta_s = \Theta_c + \frac{a'}{a} TY + TY_{|i} \gamma^i. \quad (\text{B7})$$

Inserting Eq. (B6) into this equation, we obtain

$$[\Theta_c]_{\eta_{LSS}}^{\eta_0} = [\Theta_s - \frac{a'}{a} \frac{1}{K} \mathcal{R}'_c Y - \frac{1}{K} \mathcal{R}'_c Y_{|i} \gamma^i]_{\eta_{LSS}}^{\eta_0}, \quad (\text{B8})$$

where  $[\dots]_{\eta_{LSS}}^{\eta_0}$  denotes the difference between the quantity evaluated at  $\eta_0$  and  $\eta_{LSS}$ .

On the other hand, the equation for  $\Theta_s$  is obtained from Eq. (B1) by setting  $\sigma_g = 0$  as

$$\frac{D}{d\lambda}\Theta_s = \Phi Y_{|i\gamma^i} - \Phi' Y = \frac{D}{d\lambda}(\Phi Y) - 2\Phi' Y, \quad (\text{B9})$$

where we have used the fact  $\Phi + \Psi = 0$ , which follows from Eq. (A10). Combining Eqs. (B8) and (B9), we find

$$[\Theta_c]_{\eta_{LSS}}^{\eta_0} = \left[ \Phi - \frac{a'}{a} \frac{1}{K} \mathcal{R}'_c Y - \frac{1}{K} \mathcal{R}'_c Y_{|i\gamma^i} \right]_{\eta_{LSS}}^{\eta_0} - 2 \int_{\eta_{LSS}}^{\eta_0} \Phi' Y d\lambda. \quad (\text{B10})$$

Noting that we have

$$\Phi \rightarrow \frac{3}{5} \mathcal{R}_c, \quad \frac{a'}{a} \mathcal{R}'_c \rightarrow -\frac{2}{5} \mathcal{R}_c, \quad \mathcal{R}'_c \rightarrow 0, \quad (\text{B11})$$

in the limit  $\eta \rightarrow 0$  (with  $K = -1$ ), the above equation reduces to

$$[\Theta_c]_{\eta_{LSS}}^{\eta_0} = -\frac{1}{3} \Phi Y \Big|_{LSS} - 2 \int_{\eta_{LSS}}^{\eta_0} \Phi' Y d\lambda + (\text{monopole} + \text{dipole}), \quad (\text{B12})$$

for  $\eta_{LSS} \rightarrow 0$ . This is just the formula to evaluate the CMB anisotropies due to scalar-type perturbations [31]. Thus we have proved the equivalence of the tensor and scalar approaches to the CMB anisotropies when  $p^2 = -4$ , i.e., for the wall fluctuation mode.

### APPENDIX C: ABSENCE OF THE DE SITTER SUPER-CURVATURE MODE IN THE SINGLE FIELD MODEL

Here we show there exists no discrete mode other than the wall fluctuation mode in the single field model, provided the wall thickness, i.e., the inverse mass scale of the potential is much smaller than the Hubble radius  $H^{-1}$  as well as than the wall radius  $R$ . We consider the following simplified model in which the potential in Eq. (2.18) takes the form,

$$U(\xi) = \begin{cases} U_{\text{I}} \frac{\cosh^2 \xi_0}{\cosh^2 \xi} & (\xi < \xi_0 - \varepsilon); & \text{(I)}, \\ -U_{\text{II}} & (\xi_0 - \varepsilon < \xi < \xi_0); & \text{(II)}, \\ U_{\text{III}} & (\xi_0 < \xi < \xi_0 + \varepsilon); & \text{(III)}, \\ -\frac{2}{\cosh^2 \xi} & (\xi_0 + \varepsilon < \xi < \xi_0 + \varepsilon); & \text{(IV)}, \end{cases} \quad (\text{C1})$$

where  $U_{\text{I}} := (M^2/H^2 - 2)/\cosh^2 \xi_0$  (see Fig. 10). We assume  $U_{\text{I}}, U_{\text{II}}, U_{\text{III}} \gg 1$ , in accordance with the assumption  $M^2/H^2 \gg 1$ . We note that  $\xi_0$  must be positive, since  $\dot{a}$  is negative inside the wall. We consider the solution  $\chi_p$  with  $p = i\Lambda$ , where  $0 < \Lambda \leq 2$ . Then we may approximate the potential in (I) by the constant  $U_{\text{I}}$ . Further, for simplicity, we set  $U_{\text{I}} = U_{\text{III}}$ . Then the solution takes the form,

$$\chi_\Lambda = \begin{cases} C_{\text{I}} e^{\kappa(\xi - \xi_0)} & \text{(I)}, \\ C_{\text{II}} (e^{ik(\xi - \xi_0)} + b_{\text{II}} e^{-ik(\xi - \xi_0)}) & \text{(II)}, \\ C_{\text{III}} (e^{\kappa(\xi - \xi_0)} + b_{\text{III}} e^{-\kappa(\xi - \xi_0)}) & \text{(III)}, \\ C_{\text{IV}} e^{-\Lambda(\xi - \xi_0)} (\tanh \xi + \Lambda) & \text{(IV)}, \end{cases} \quad (\text{C2})$$

where

$$\kappa = \sqrt{U_{\text{I}} + \Lambda^2}, \quad k = \sqrt{U_{\text{II}} - \Lambda^2}, \quad (\text{C3})$$

and  $C$ 's and  $b$ 's are constants determined by the continuity conditions of  $\chi_\Lambda$  and  $d\chi_\Lambda/d\xi$ . In (I), we take only the growing solution ( $\propto e^{\kappa\xi}$ ) because the contribution from the decaying solution ( $\propto e^{-\kappa\xi}$ ) will be exponentially suppressed.

Solving the continuity condition of  $d(\ln \chi_\Lambda)/d\xi$  at  $\xi = \xi_0 - \varepsilon$  and  $\xi = \xi_0$ , we find  $d(\ln \chi_\Lambda)/d\xi$  at  $\xi = \xi_0 + \varepsilon$  is calculated from the left of the point to be

$$\psi_L := \kappa \frac{\sin(2\theta - k\varepsilon)e^{\kappa\varepsilon} - \sin \kappa\varepsilon e^{-\kappa\varepsilon}}{\sin(2\theta - k\varepsilon)e^{\kappa\varepsilon} + \sin \kappa\varepsilon e^{-\kappa\varepsilon}}, \quad (\text{C4})$$

where

$$\tan \theta = \kappa/k. \quad (\text{C5})$$

On the other hand, the same quantity is calculated from the right of  $\xi_0 + \varepsilon$  to be

$$\psi_R := -\Lambda + \frac{1}{\cosh^2(\xi_0 + \varepsilon)(\tanh(\xi_0 + \varepsilon) + \Lambda)}. \quad (\text{C6})$$

Thus the continuity condition at  $\xi = \xi_0 + \varepsilon$  reduces to

$$\psi_L = \psi_R. \quad (\text{C7})$$

This equation must be satisfied for  $\Lambda = 2$  because we know the wall fluctuation mode always exists. This condition gives one constraint on the model parameters  $U_I, U_{II}$  and  $\varepsilon$ . Therefore all of them cannot be chosen arbitrarily. This reflects the fact that  $\mathcal{M}^2 = V''(\sigma_B)$ . Suppose we fix  $U_I$  and  $U_{II}$ , or equivalently,  $\tilde{\kappa} := \kappa|_{\Lambda=2}$  and  $\tilde{k} := k|_{\Lambda=2}$ . Then  $\varepsilon$  is determined from Eq. (C7) with  $\Lambda = 2$ . In order to find the order of magnitude of  $\varepsilon$ , we note that  $-2 < \psi_R < -3/2$  when  $\Lambda = 2$ , i.e.  $\psi_R = O(1)$ . Since  $\kappa \gg 1$ , this implies the numerator in  $\psi_L$  must be small,

$$\sin(2\tilde{\theta} - \tilde{k}\varepsilon)e^{\tilde{\kappa}\varepsilon} - \sin \tilde{\kappa}\varepsilon e^{-\tilde{\kappa}\varepsilon} \ll 1, \quad (\text{C8})$$

where  $\tilde{\theta} = \theta|_{\Lambda=2}$ . Thus we find that  $\varepsilon = O(1/\kappa)$ . Using the above inequality, the denominator in  $\psi_L$  is evaluated for  $\Lambda = 2$  as

$$\sim 2 \sin \tilde{\kappa}\varepsilon e^{-\tilde{\kappa}\varepsilon}, \quad (\text{C9})$$

and is of order unity.

Now we show that no other discrete mode exists. Suppose there existed another discrete mode. The next largest eigenvalue solution must have one node. Noting the constraints  $\xi_0 > 0$  and  $\Lambda > 0$ , we can easily see that there would be no node in (IV). Thus the solution must have a node in (II) or (III). As we decrease  $\Lambda$  from 2, because  $\chi_\Lambda$  must vanish at  $\xi = \xi_0 + \varepsilon$  just before a node would first appear in (III),  $\psi_L$  would diverge for some value of  $\Lambda$ . However, the changes of  $k$  and  $\kappa$  due to the variation of  $\Lambda$  would be at most of  $O(1/\tilde{k})$  and  $O(1/\tilde{\kappa})$ , respectively, and accordingly the change of  $\theta$  would be also small. Hence there is no chance that the denominator in  $\psi_L$  would vanish, which is a contradiction. Thus we conclude that there is no discrete mode other than the wall fluctuation mode in this limiting case.

- [1] P.J.E. Peebles, *Principle of Physical Cosmology*, (Princeton Univ. Press, 1993).
- [2] B. Ratra and P.J.E. Peebles, *AstroPhys. J.* **432**, L5 (1994).
- [3] J.R. Primack, in *Snoumass 94*, eds. E.W. Kolb and R.D. Peccei, (World Scientific, 1995).
- [4] M. Bucher, A.S. Goldhaber and N. Turok, *Nucl. Phys. B*, Proc. Suppl. **43**, 173 (1995); M. Bucher, and N. Turok, *Phys. Rev. D* **52**, 5538 (1995).
- [5] K. Yamamoto, M. Sasaki and T. Tanaka, *Astrophys. J.* **455**, 412 (1995).
- [6] A.D. Linde, *Phys. Lett. B* **351**, 99 (1995).
- [7] A.D. Linde and A. Mezhlumian, *Phys. Rev. D* **52**, 5538 (1995).
- [8] S. Coleman, *Phys. Rev. D* **15**, 2929 (1977).
- [9] S. Coleman and F. De Luccia, *Phys. Rev. D* **21** 3305 (1980).
- [10] K. Yamamoto, T. Tanaka, and M. Sasaki, *Phys. Rev. D* **51**, 2968 (1995).
- [11] T. Hamazaki, M. Sasaki, T. Tanaka, and K. Yamamoto, *Phys. Rev. D* **53** 2045 (1996).
- [12] M. Sasaki, T. Tanaka, and K. Yamamoto, *Phys. Rev. D* **51**, 2979 (1995).
- [13] K. Yamamoto and E.F. Bunn, preprint KUNS-1357, *Astrophys. J.* (1996) in press.
- [14] J. Garriga, preprint UAB-FT-387, gr-qc/9602025 (1996).
- [15] J. Garcia-Bellido, preprint SUSSEX-AST 95/10-1, astro-ph/9510029 (revised version) (1996).
- [16] T. Tanaka, M. Sasaki, and K. Yamamoto, *Phys. Rev. D* **49**, 1039 (1994).
- [17] T. Tanaka and M. Sasaki, *Phys. Rev. D* **50**, 6444 (1994).
- [18] V.A. Rubakov, *Nucl. Phys. B* **245**, 481 (1984).

- [19] H.E. Kandrup, Phys. Lett. B **225**, 222 (1989); Phys. Rev. D **42**, 3401 (1990).
- [20] T. Vachaspati and A. Vilenkin, Phys. Rev. D **43**, 3846 (1991).
- [21] M. Sasaki, T. Tanaka, K. Yamamoto, and J. Yokoyama, Prog. Theor. Phys. **90**, 1019 (1993); Phys. Lett. B **317**, 510 (1993).
- [22] J.L. Gervais and B. Sakita, Phys. Rev. D **15** 3507 (1977).
- [23] D. Lyth and A. Woszczyna, Phys. Rev. D **52** 3338 (1995).
- [24] J. Garcia-Bellido, A. Liddle, D. Lyth, and D. Wands, Phys. Rev. **D52**, 6750 (1995).
- [25] W. Magnus, F. Oberhettinger, and R.P. Soni, *Formulas and Theorems for the Special Functions of Mathematical Physics*, Springer-Verlag, Berlin, (1966).
- [26] C. G. Callan, and S. Coleman, Phys. Rev. D **16**, 1762 (1977).
- [27] D.H. Lyth and E.D. Stewart, Phys. Lett. B **252**, 336 (1990).
- [28] B. Ratra and P.J.E. Peebles, Phys. Rev. D **52**, 1837 (1995).
- [29] M. Kamionkowski, B. Ratra, D.N. Spergel, and N. Sugiyama, Astrophys. J. **434**, L1 (1994).
- [30] K.M. Gorski, B. Ratra, N. Sugiyama, and A.J. Banday, Astrophys. J. **444**, L65 (1995).
- [31] N. Gouda, N. Sugiyama and M. Sasaki, Prog. Theor. Phys. **85**, 1023 (1991).
- [32] H. Kodama and M. Sasaki, Prog. Theor. Phys. Suppl. **78**, 1 (1984).
- [33] S.W. Hawking and I.G. Moss, Phys. Lett., **110B**, 35 (1982).
- [34] S. Coleman, *Aspects of Symmetry*(Cambridge University Press, Cambridge, England, 1985),
- [35] S. Coleman, V. Glaser and A. Martin, Commun. Math. Phys., **58**, 211 (1978).
- [36] T. Tanaka and M. Sasaki, Prog. Theor. Phys., **88**, 503 (1992).
- [37] S. Parke, Phys. Lett. B **121**, 313 (1983).
- [38] C.L. Bennett et al., Astrophys. J. **436**, 423 (1994).

### Figure Captions

Figure 1. A schematic picture of the tunneling potential for the one-bubble open inflationary scenario, (a) for a single field model and (b) for a two-field model.

Figure 2. Penrose diagram of the de Sitter space. The coordinates which cover the regions R, L and C are shown, respectively.

Figure 3. A schematic picture of  $\mathcal{M}^2$  as a function of  $\tau$  ( $= t_C$ ) in the case of a single field model.

Figure 4. The power spectrum of CMB anisotropies due to the wall fluctuation mode for various values of  $\Omega_0$ . The lines are normalized by  $H^2/(S_1 R)$ .

Figure 5. A schematic picture of  $U(\xi)$  in eq.(2.19) for a two-field model with thin-wall approximation.

Figure 6. The power spectra of curvature perturbations due to the continuous modes. The real line, the long dashed line, the short dashed line and the dotted line are, respectively, for  $HR = 0.1, 0.5, 0.7$  and  $0.9$ , for (a)  $M/H = 2$  and (b)  $M/H = 10$ .

Figure 7. The eigenvalue  $\Lambda$  of the de Sitter super-curvature mode as a function of  $HR$  where  $R$  is the wall radius. The three lines, from top to bottom, show the cases for  $M^2/H^2 = 5/4, 2$  and  $9/4$ , where  $M$  is the mass outside the bubble.

Figure 8. The critical line on which the de Sitter super-curvature mode disappears on the  $(M/H, HR)$ -plane. The super-curvature mode exists in the region below the line.

Figure 9. The CMB anisotropy power spectra in the open universe with  $\Omega_0 = 0.1$  predicted in two-field models. The lines are normalized by  $(3H^2/5\phi_B)^2$ . The top and the bottom curves are the results when the scalar field is in the Bunch-Davies vacuum and the conformal vacuum, respectively. For the other lines, the model parameters are  $M^2/H^2 = 2$  and  $HR = 0.9, 0.7, 0.5$ , and  $0.3$ , from top to bottom.

Figure 10. A simplified potential  $U(\xi)$  for a single field model.

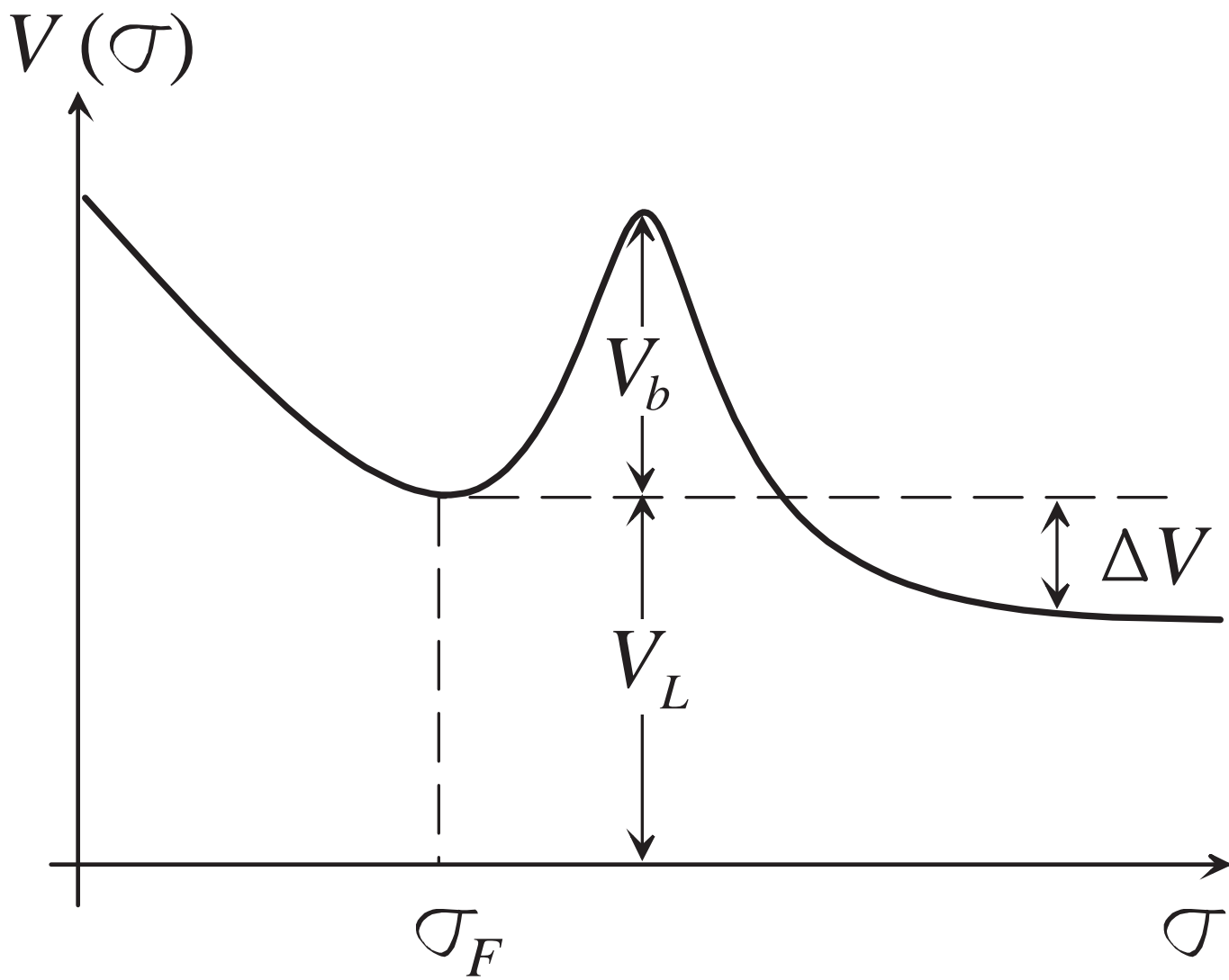


Fig. 1(a)

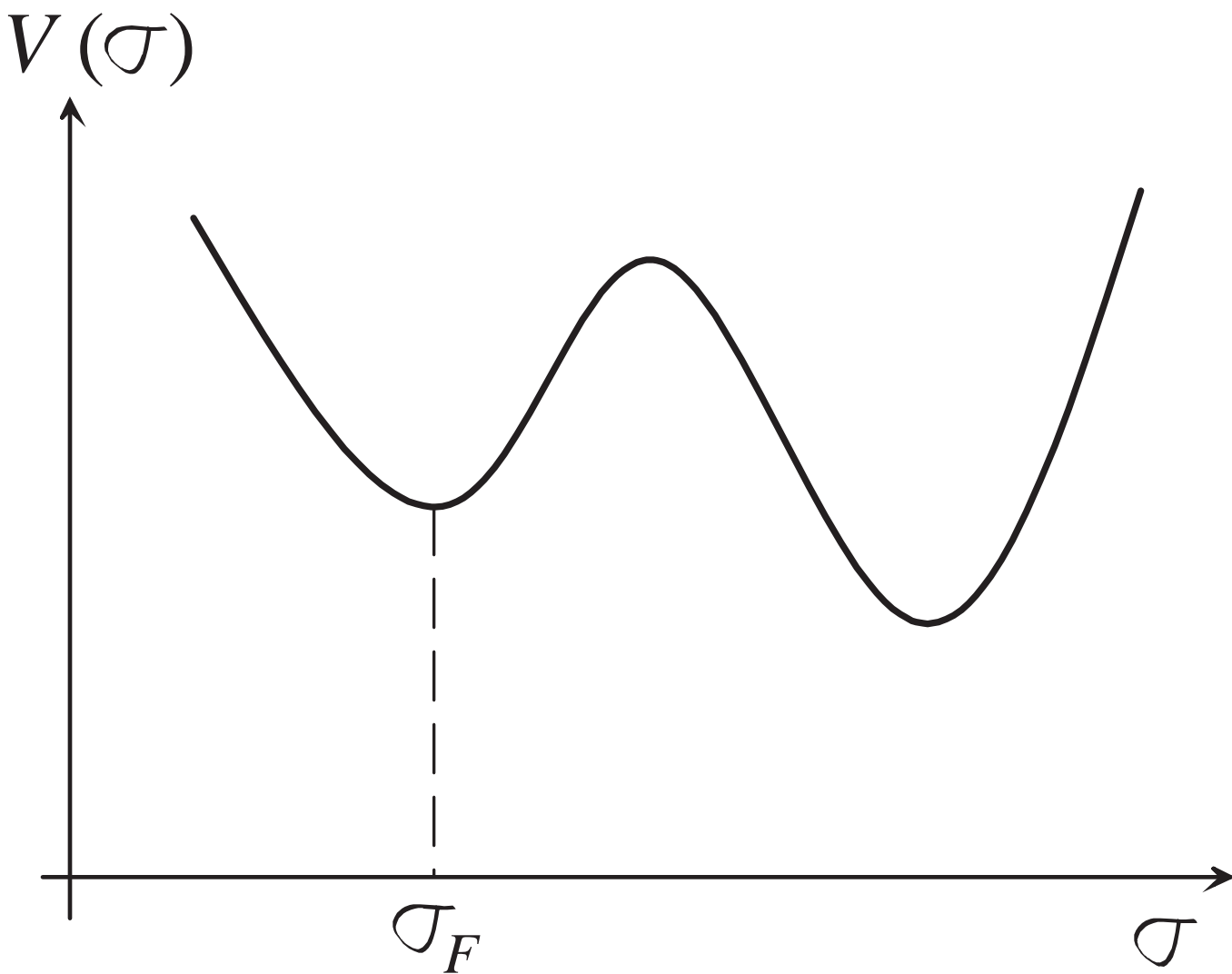


Fig. 1(b)



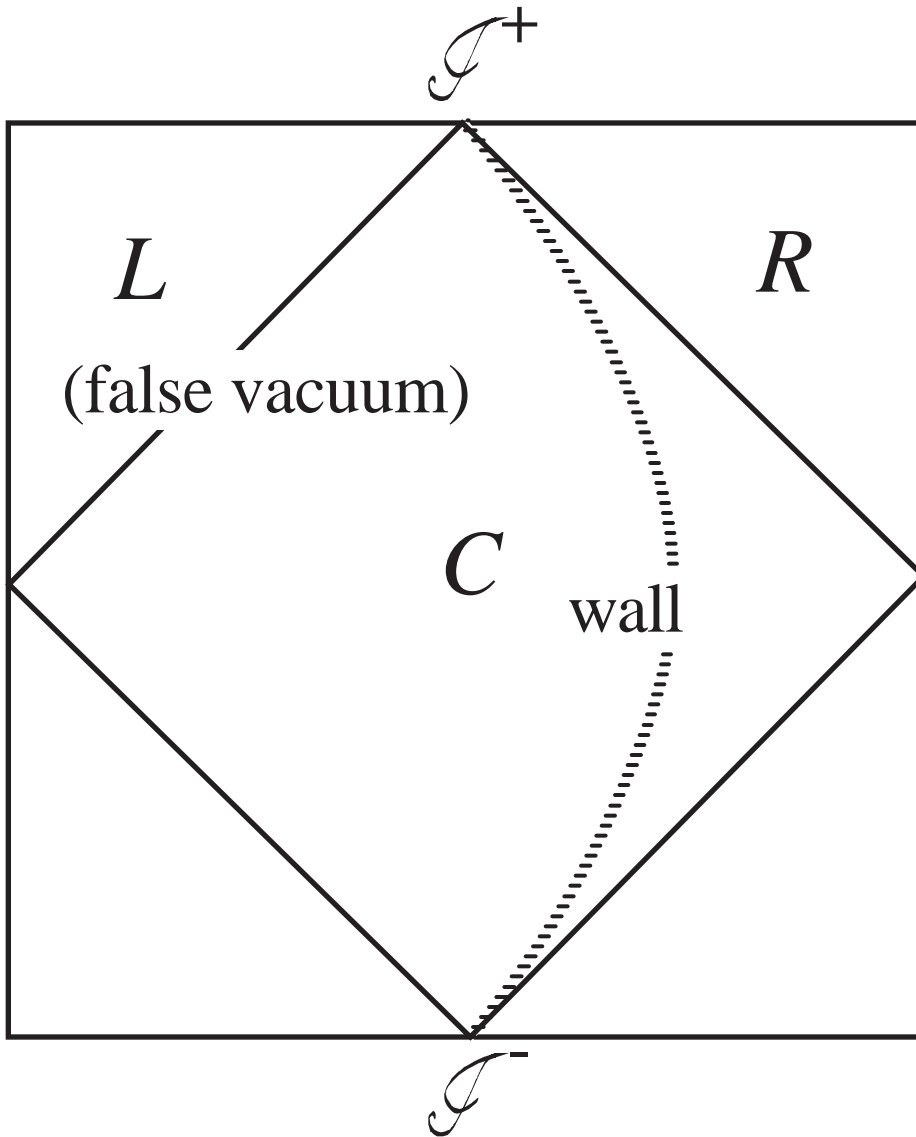


Fig. 2

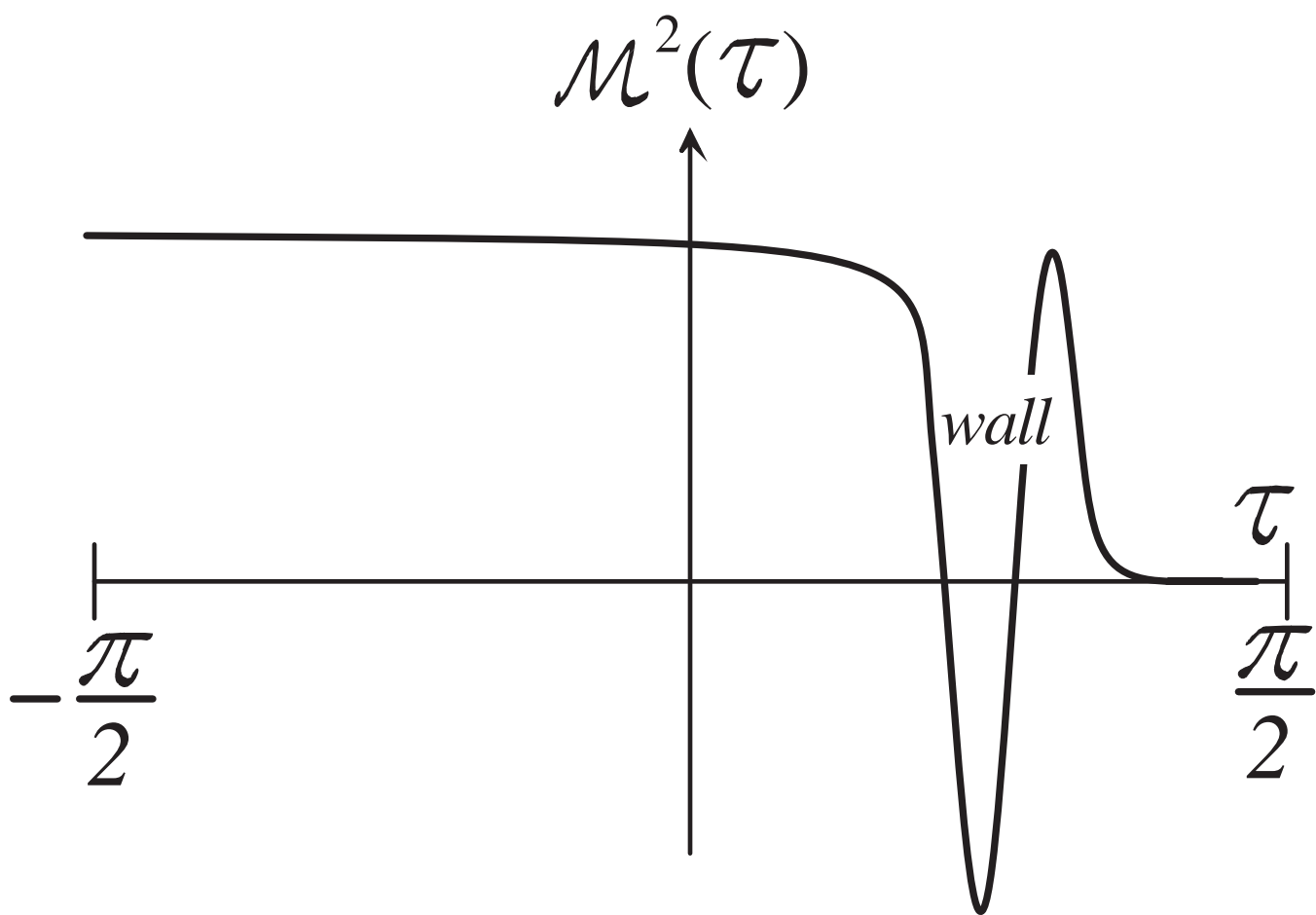


Fig. 3

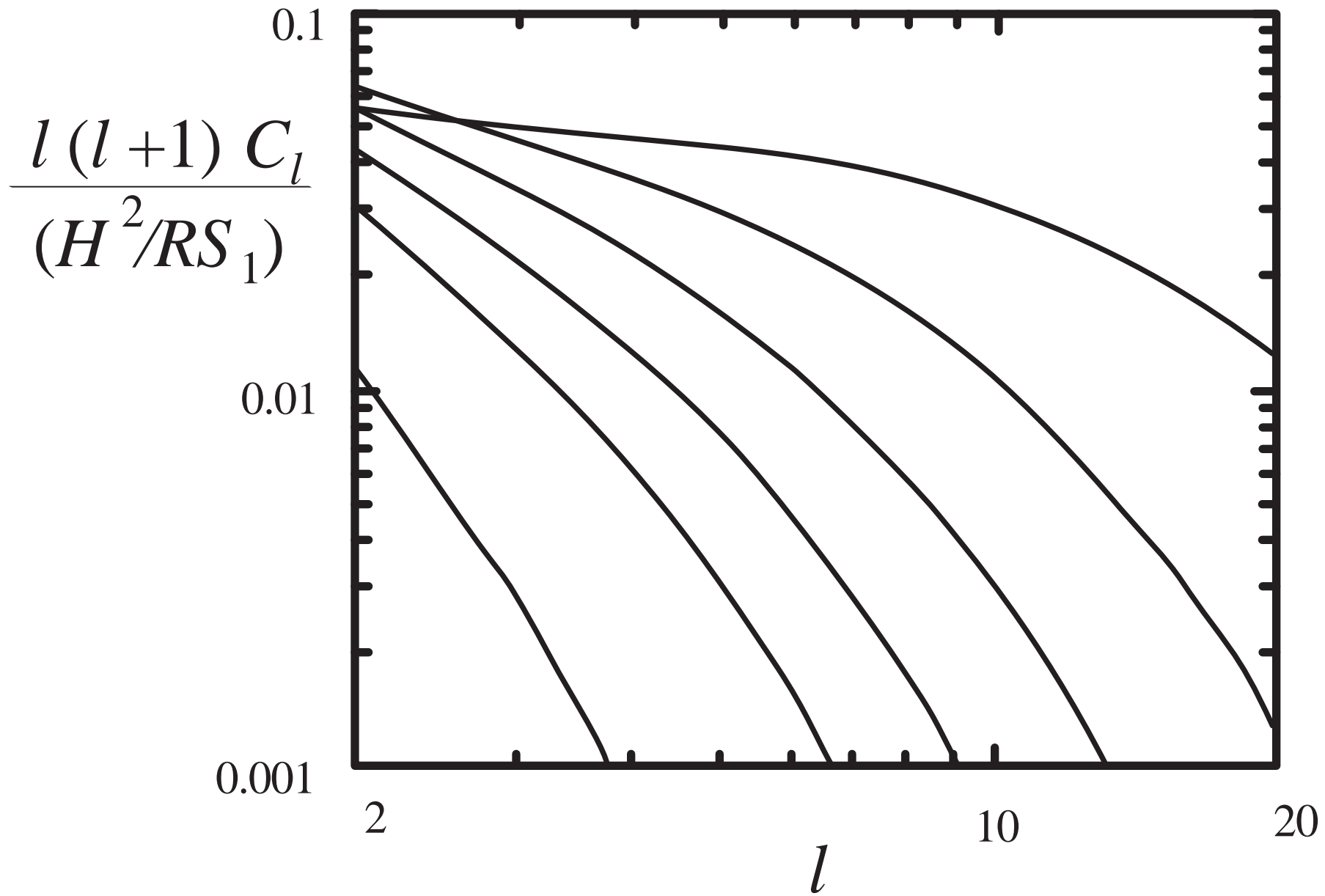


Fig. 4

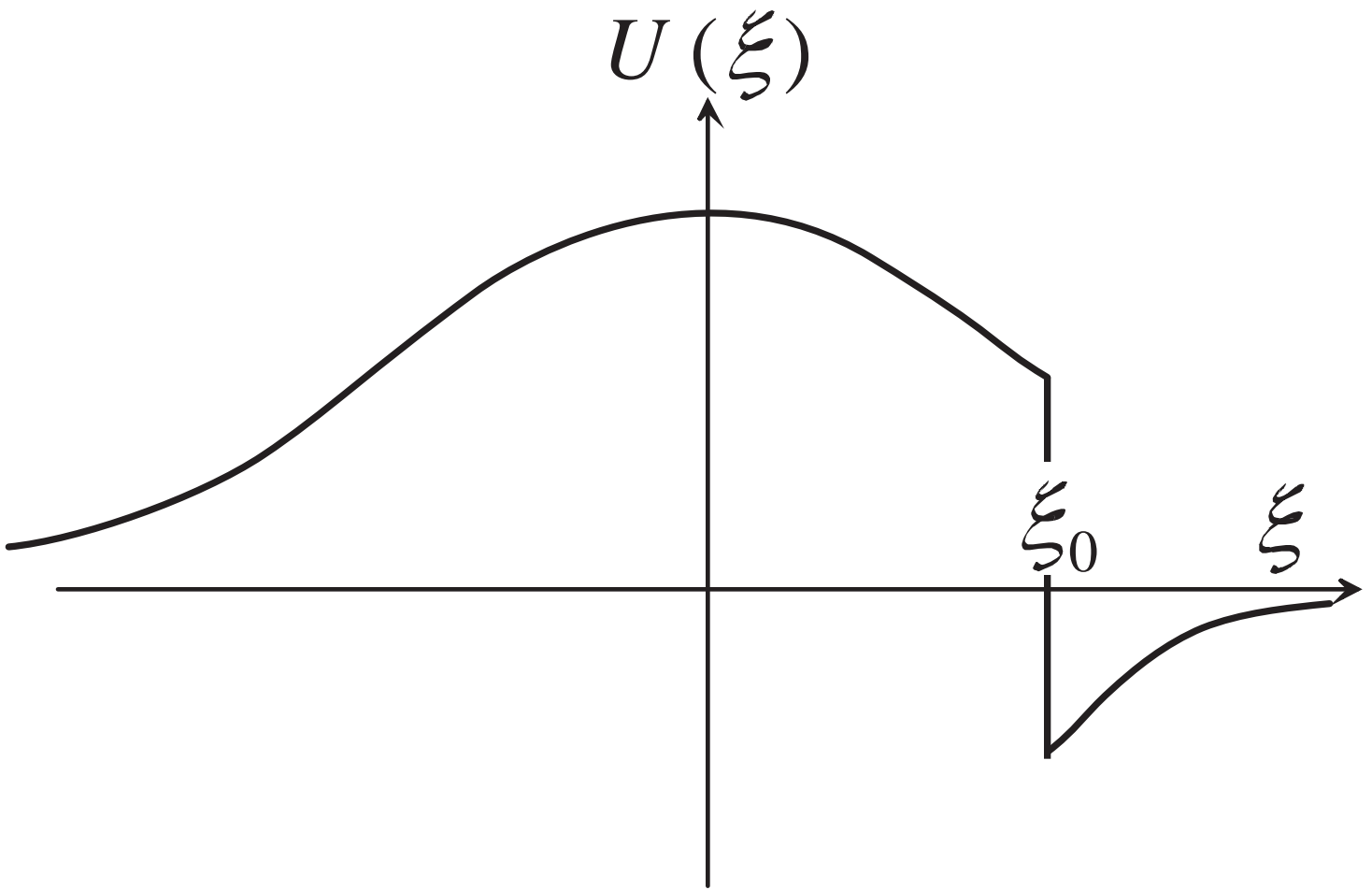


Fig. 5

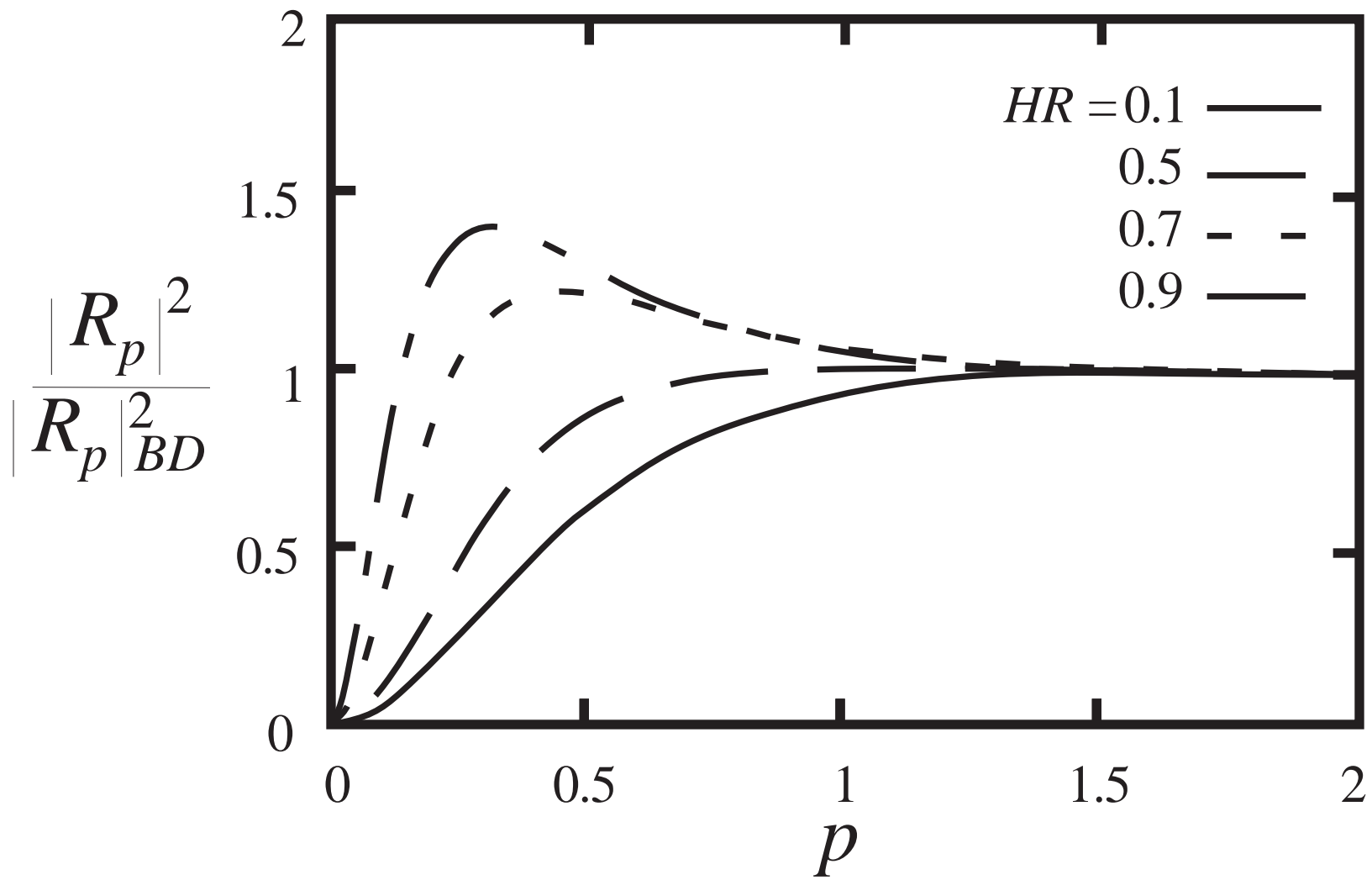


Fig. 6(a)

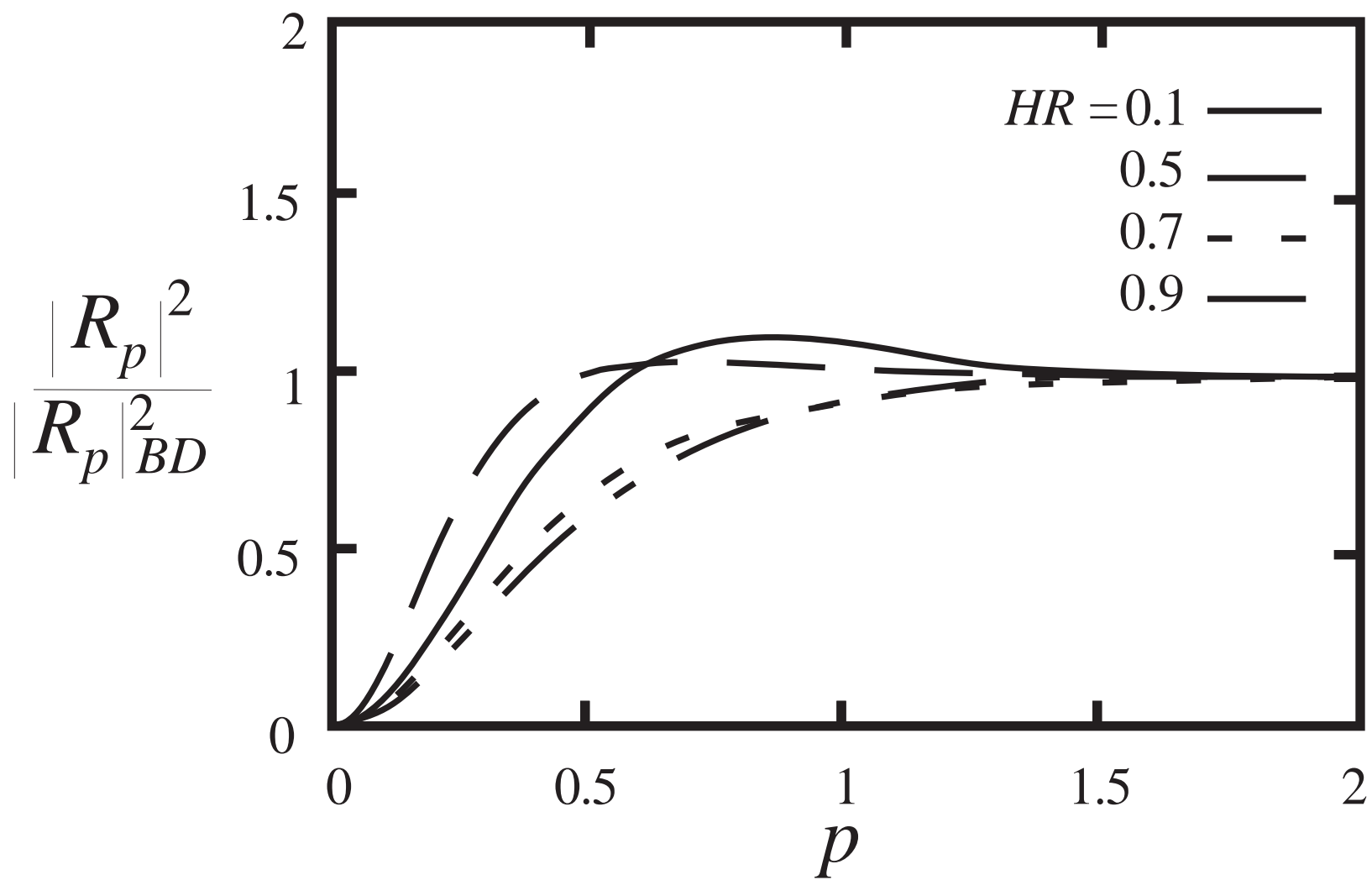


Fig. 6(b)

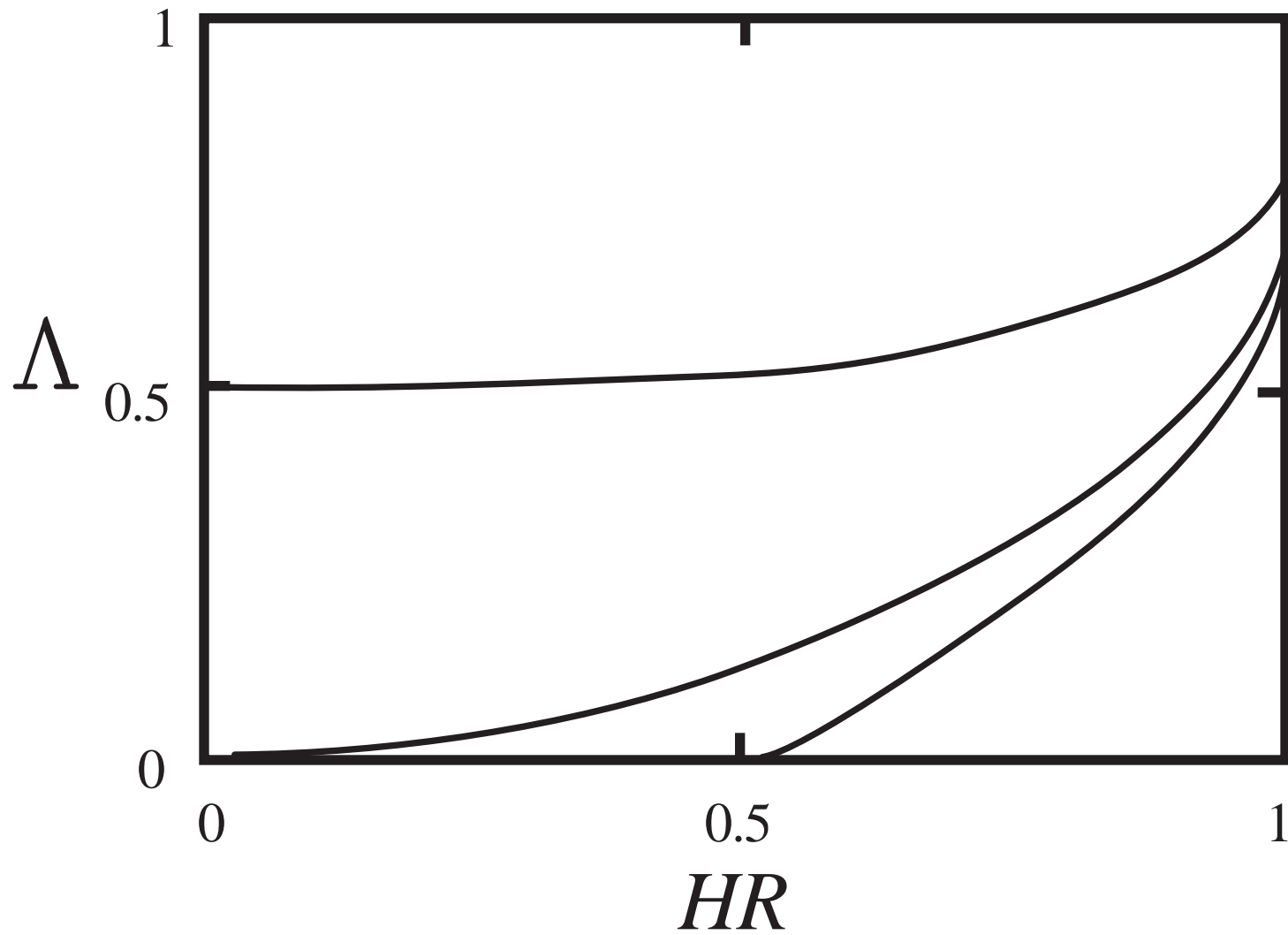


Fig. 7

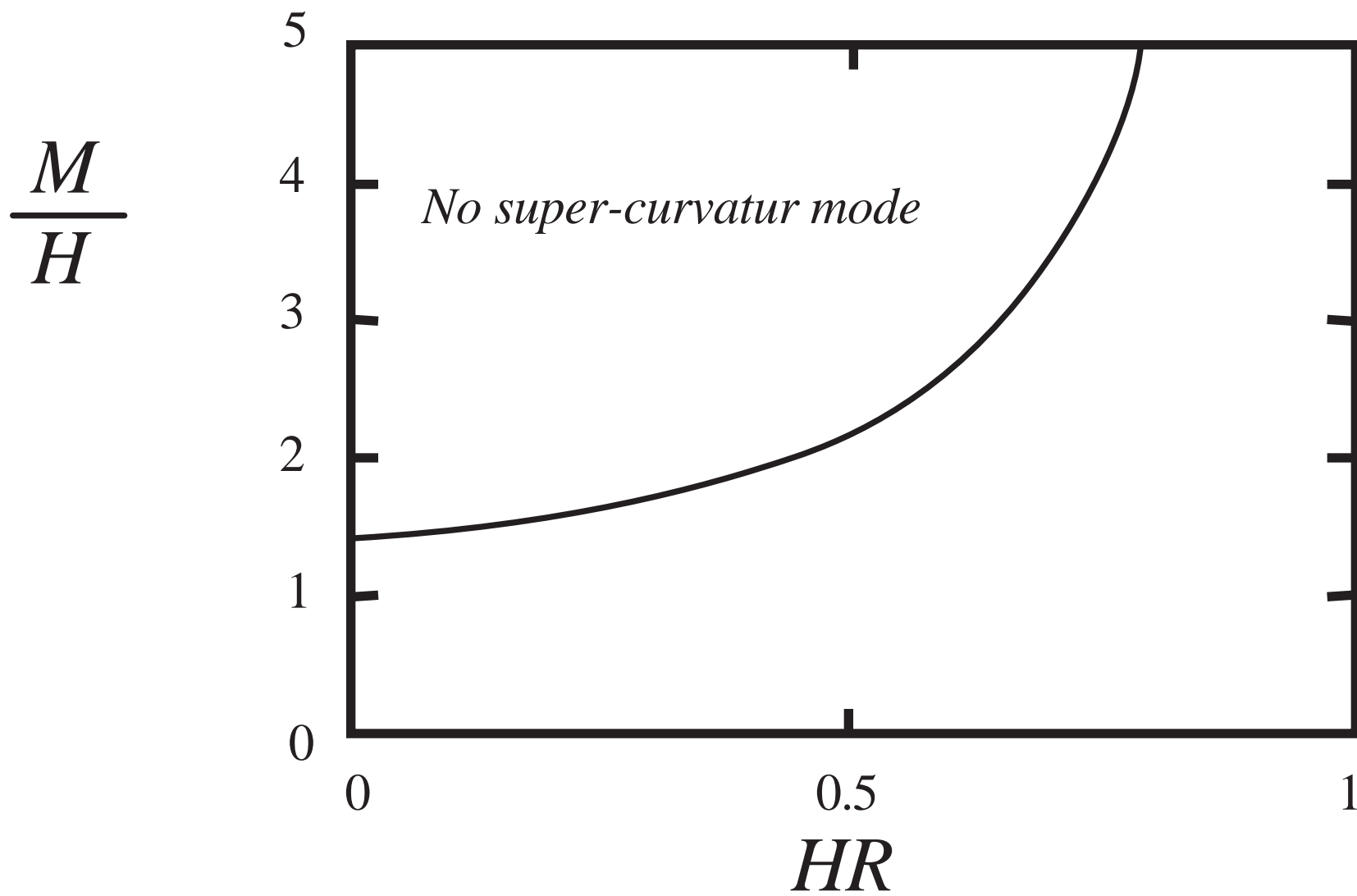


Fig. 8



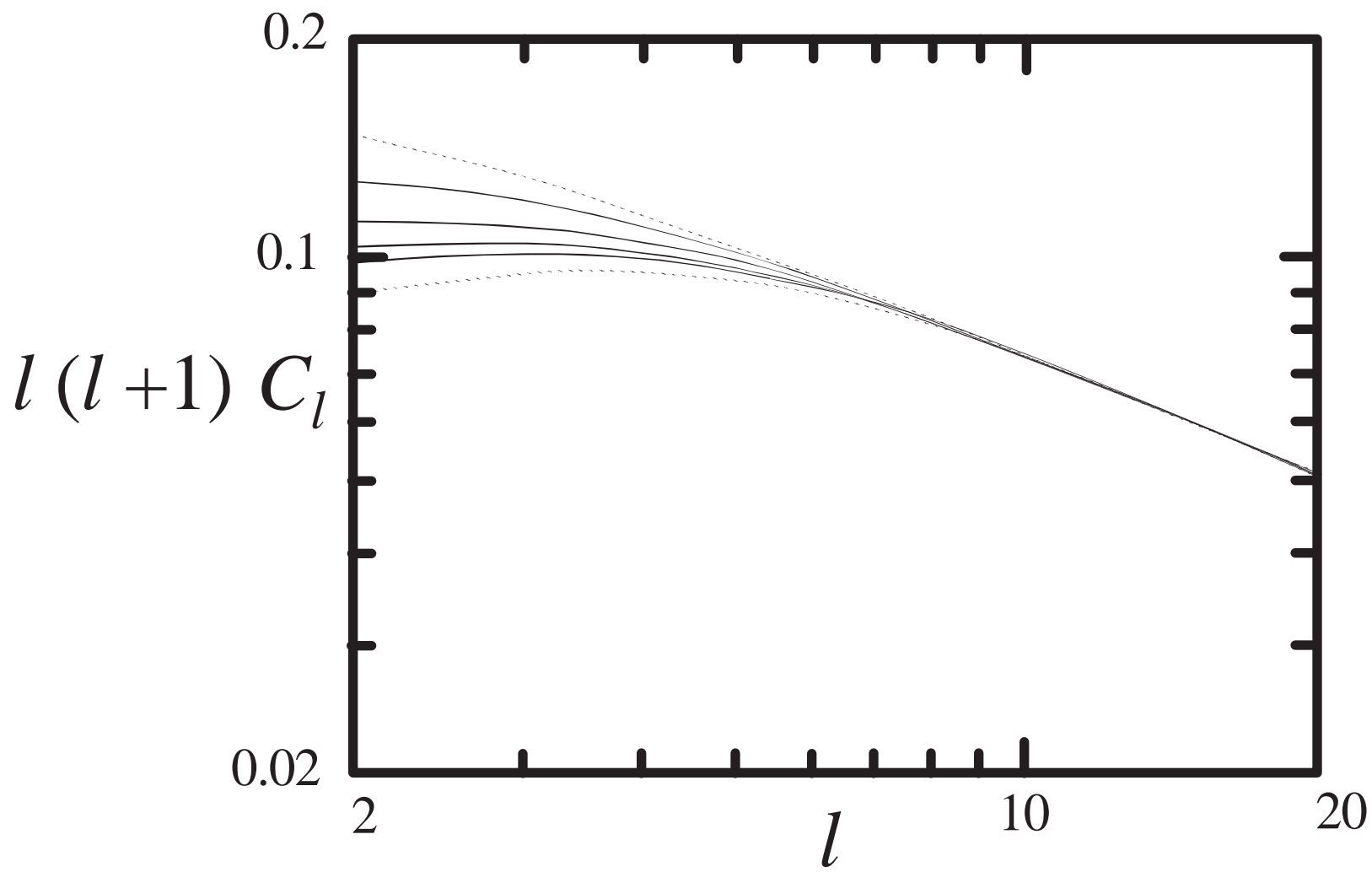


Fig. 9

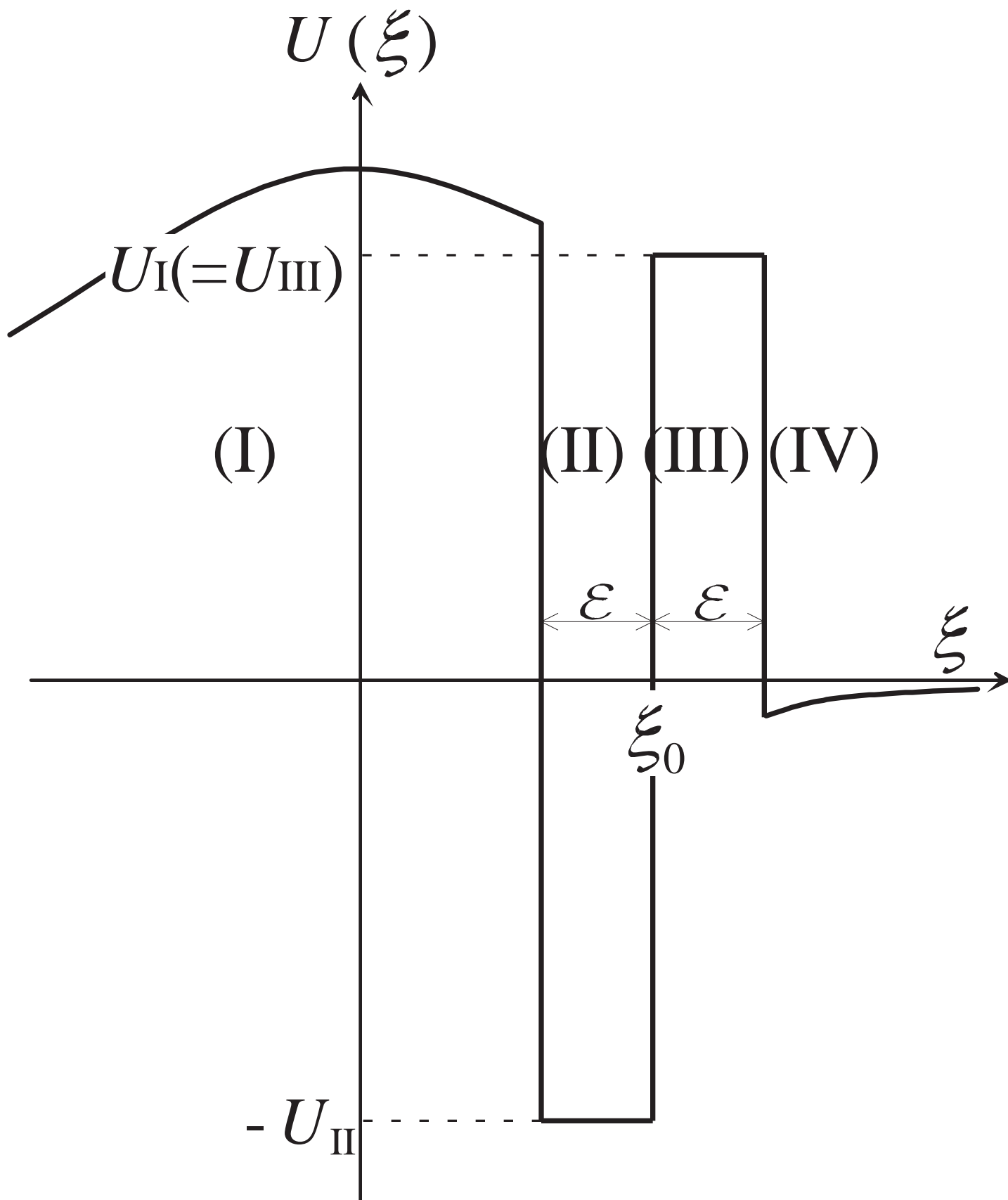


Fig. 10